Electronic Supporting Information

Chain Length Effect on the Structural and Emission Properties of the CuI/Bis((4-methoxyphenyl)thio)-alkane Coordination Polymers

*Adrien Schlachter**,[1] Rebecca Scheel,[2] Daniel Fortin,[1] Carsten Strohmann,[2] Michael Knorr[3]* and Pierre D. Harvey[1]**

[1]Département de Chimie, Université de Sherbrooke 2550 Boulevard Université, Sherbrooke, PQ, Canada, J1K 2R1.

[2]Anorganische Chemie, Technische Universität Dortmund, Otto-Hahn-Straße 6, 44227 Dortmund, Germany.

[3]Institut UTINAM, UMR CNRS 6213, Université Bourgogne Franche-Comté, 16, Route de Gray, 25030 Besançon, France.

Corresponding Author

*E-mail: Adrien.Schlachter@USherbrooke.ca (A.S.)

*E-mail: Pierre.Harvey@USherbrooke.ca (P.D.H.)

*E-mail: Michael.Knorr@univ-fcomte.fr (M.K.).

Table of Content

Experimental Section

Instrumentation

Single Crystal X-ray Structure Analyses: Single crystals of **CP2** and **CP8** were mounted on a Bruker D8 Venture four-circle diffractometer equipped with a nitrogen jet stream low-temperature system (Oxford Cryosystems). The X-ray source was graphite monochromated Mo-Kα radiation (λ = 0.71073 Å) from a microfocus sealed tube IμS by Incoatec. The lattice parameters were obtained by least-squares fit to the optimized setting angles of the entire set of collected reflections. Intensity data were recorded as ϕ and ω scans with κ offsets. No significant intensity decay or temperature drift was observed during data collections. Data were reduced by using SAINT v8.37A (Bruker, 2015) software and absorption correction was carried out by SADABS-2016/2 (Bruker, 2016). The structure was solved using SHELXT (Sheldrick, 2015) with intrinsic phasing. Refinements were carried out by full-matrix least-squares on F2 using SHELXL program (Sheldrick, 2015) on the complete set of reflections. All non–hydrogen atoms were refined with anisotropic thermal parameters, whereas the H atoms were treated in a riding mode.[1–3]

Single crystals of **CP3**, **CP5** and **CP6** were mounted on a Bruker APEX-II DUO equipped with a nitrogen jet stream low-temperature system (Oxford Cryosystems). The X-ray source was from graphite monochromated Mo-Kα radiation (λ = 0.71073 Å) sealed tube or Cu (λ = 1.54186 Å) microfocus tube IμS with MX optics by Incoatec. The lattice parameters were obtained by least-squares fit to the optimized setting angles of the entire set of collected reflections. Intensity data were recorded as ϕ and ω scans. Data were reduced by using SAINT v8.37A (Bruker, 2015) software and absorption correction was carried out by SADABS-2016/2 (Bruker, 2016). The structure was solved using the Bruker SHELXTL Software Package. Refinement was performed with shelxl-crystal structure refinement-multi-cpu version, George M. Sheldrick 1993-2018 version 2018/3 on the complete set of reflections. All non–hydrogen atoms were refined with anisotropic thermal parameters.[2,3]

A/B level alerts: CP3: No omission or oversight. These alerts are caused by a very large unit cell difficult to handle by checkcif routine. All data, R, Goodness of fit, are very satisfying for a structure of this size. **CP5**: This is caused by disordered part # in refinement that do not converge. All other refinement parameters are good.

Powder XRD measurements: The samples for powder XRD measurements were mixed with a small amount of paratone oil, cut to approximately 0.3 × 0.3 × 0.3 mm^3, and placed on a sample

holder mounted at 173.2 K on a Bruker APEX DUO X-ray diffractometer. Six correlated runs per sample with Phi Scan of 360 degrees and exposure times of 270 s were collected with the Cu micro-focus anode (1.54184 Å) and the CCD APEX II detector at a 150 mm distance. These runs, from −12 to −72°2θ and 6 to 36ω, were then treated and integrated with the XRW2 Eval Bruker software to produce WAXD diffraction patterns from 2.5 to 82°2θ. The patterns were treated with Diffrac.Eva version 2.0 from Bruker.

Structure of **CP7**. The structure of **CP7** was elucidated from computer modeling and simulation of the powder X-ray diffraction (PXRD) pattern by comparison with the experimental pattern. Simulations of the PXRD using Treor90[4] and the FullProf Suite.[4,5] A reliable structure was computed and found to be in good agreement with experimental data with a percentage of similarity with compensation for background and baseline discrepancies (Rwp(w/o bck) at 98.7%.

Elemental analysis: The elemental analysis were performed by the analytical service of the University of Lorraine in Nancy, France.

NMR: The ^{1}H (300 MHz) and ^{13}C (76 MHz) NMR spectra were recorded on a Bruker Avance 300 Ultrashield NMR spectrometer. The chemical shifts are given in ppm relative to the residual peaks of $CDCl_3$.

Thermal analysis: The thermal analysis (TGA) traces were measured on a Perkin Elmer TGA 7 apparatus in the temperature range between 25 and 950 °C at a scanning rate of 10°C.min^{-1} under argon atmosphere.

FT-Raman: The FT-Raman spectra were recorded from 0 to 4000 cm^{-1}, at 5 cm^{-1} resolution using a Bruker RFS 100/S spectrometer with the 1064 nm excitation and a light power equal to 250 mW equipped with a photomultiplier Ge-diode, cooled at liquid nitrogen temperature (77 K). The peak centred between 83 and 85 cm^{-1} is considered as residual artefact from the instrument and shouldn't be considered.

FT-IR: The IR spectra were recorded at 4 cm^{-1} on an ABB Bomem, MB series FTIR spectrometer equipped with an ATR module from Specac from 600 to 4000 cm^{-1}.

Photophysical instrumentation: The solid-state UV-visible spectra were recorded on a Varian Cary 300 Bio UV-Vis spectrophotometer at 298 K using raised-angle transmittance apparatus and a homemade 77 K sample-holder. Samples were dispersed between two quartz plates. Solid-state emission, excitation, emission lifetimes and CIE 1931 charts (chromaticity

coordinates) were acquired on a phosphorimeter FLS980 from Edinburgh Instruments equipped with single monochromators. Samples were introduced in a capillary or dispersed between two quartz plates and spectra obtained were corrected for instrument response. The emission lifetime measurements were performed using a "flash" pulsed lamp. Lifetimes values were obtained using a time correlated single photon counting (TCSPC) system and data were treated from both deconvolution of multi-exponential analysis and exponential series method. Solid state emission quantum yields were recorded using a Quanta-φ F-3029 integration sphere from Horiba plugged into a Horiba Fluorolog III.

Synthesis

Materials. CuI, 4-methoxythiophenol and corresponding dihalogeno alkane $X(CH_2)_mX$ (m = 2-8, X = I, Br) were purchased from Acros, Millipore Sigma and Oakwood Chemicals and used without further purifications. All reactions were performed using standard Schlenk techniques.

General procedure for ligands synthesis. The ligands bis(4-methoxyphenylthio)alkane were prepared using a modified literature procedure.[6,7] 2 equivalents of 4-methoxythiophenol was deprotonated in an EtOH solution of 1.1 equivalent of KOH. After stirring 1h, the corresponding alkyl dihalide (1 equivalent) was added dropwise. Stirring was continued for 1h and then the mixture was refluxed for 1h. After separation of precipitated KCl (or KBr), the solvent was evaporated, the residue was washed with water and extracted with CH_2Cl_2. Recrystallisation in ethanol affords most of the ligands after storing at -20°C in form of colorless or pale yellowish crystal, which melt reaching ambient temperature to produce viscous oils, except **L2**, which remains solid.

Bis(4-methoxyphenylthio)ethane L2. ^{1}H NMR (300 MHz, $CDCl_3$): δ (ppm): 7.23 – 7.20 (m, 4H; ArH), 6.76 – 6.73 (m, 4H; ArH), 3.72 (6H; s, CH_3O), 2.86 (s, 4H; CH_2); ^{13}C NMR (101 MHz, $CDCl_3$): δ (ppm): 159.18, 133.70, 125.16, 114.64, 55.37, 35.25.

Bis(4-methoxyphenylthio)propane L3. ^{1}H NMR (300 MHz, $CDCl_3$): δ (ppm): 7.32 – 7.29 (m, 4H, ArH), 6.83 – 6.80 (m, 4H, ArH), 3.79 (6H; s, CH_3O), 2.93 – 2.88 (t, 4H; CH_2), 1.86 – 1.76 (quint, 2H; CH_2); ^{13}C NMR (76 MHz, $CDCl_3$): δ (ppm): 159.15, 133.60, 126.24, 114.72, 55.47, 34.71, 28.79.

Bis(4-methoxyphenylthio)pentane L5. ^{1}H NMR (300 MHz, $CDCl_3$): δ (ppm): 7.34 – 7.31 (m, 4H, ArH), 6.85 – 6.82 (m, 4H, ArH), 3.79 (6H; s, CH_3O), 2.81 – 2.76 (t, 4H; CH_2), 1.61 – 1.48 (m, 6H; CH_2); ^{13}C NMR (76 MHz, $CDCl_3$): δ (ppm): 158.99, 133.23, 126.84, 114.69, 55.48, 35.83, 29.01, 27.77.

Bis(4-methoxyphenylthio)hexane L6. ^{1}H NMR (300 MHz, $CDCl_3$): δ (ppm): 7.34 – 7.31 (m, 4H, ArH), 6.85 – 6.82 (m, 4H, ArH), 3.79 (6H; s, CH_3O), 2.82 – 2.77 (t, 4H; CH_2), 1.59 – 1.54 (m, 4H; CH_2), 1.41 – 1.36 (m, 4H; CH_2); ^{13}C NMR (76 MHz, $CDCl_3$): δ (ppm): 158.93, 133.12, 126.97, 114.66, 55.47, 35.89, 29.33, 28.32.

Bis(4-methoxyphenylthio)heptane L7. ^{1}H NMR (300 MHz, $CDCl_3$): δ (ppm): 7.34 – 7.31 (m, 4H, ArH), 6.85 – 6.82 (m, 4H, ArH), 3.79 (6H; s, CH_3O), 2.82 – 2.77 (t, 4H; CH_2), 1.59 – 1.54 (m, 4H; CH_2), 1.40 – 1.26 (m, 6H; CH_2); ^{13}C NMR (76 MHz, $CDCl_3$): δ (ppm): 158.85, 133.05, 126.97, 114.61, 55.44, 35.88, 29.35, 28.81, 28.63.

Bis(4-methoxyphenylthio)octane L8. ^{1}H NMR (300 MHz, $CDCl_3$): δ (ppm): 7.34 – 7.31 (m, 4H, ArH), 6.85 – 6.82 (m, 4H, ArH), 3.79 (6H; s, CH_3O), 2.82 – 2.77 (t, 4H; CH_2), 1.61 – 1.51 (m, 4H; CH_2), 1.39 – 1.35 (m, 4H; CH_2), 1.27 – 1.25 (m, 4H; CH_2); ^{13}C NMR (76 MHz, $CDCl_3$): δ (ppm): 158.85, 133.04, 127.03, 114.62, 55.46, 35.93, 29.42, 29.15, 28.72.

General procedure for the synthesis of the CPs: All CuI-based CPs were prepared in a similar manner as previously described for the preparation of $[Cu_4I_4\{\mu\text{-}ArS(CH_2)_nSAr\}_2]_n$ and $[\{Cu(\mu_2\text{-}I)_2Cu\}\{\mu\text{-}ArS(CH_2)_nSAr\}_2]_n$ [8,9] by mixing at ambient temperature CuI with the corresponding dithioether using MeCN as solvent. To avoid formation of product mixtures, it is preferential to obtain the pure compound by adding 1 equivalent of the appropriate ligand to a clear solution of two equivalents of CuI in MeCN. Partial precipitation of the white polymer occurred shortly after addition. The precipitate was the refluxed for 2-3 min until all material redissolved (sometimes by addition of an additional amount of solvent), the solution was allowed to reach slowly room temperature to yield the targeted product in crystalline form.

Polymer CP2. Yield (78%) Anal. Calcd. for $C_{16}H_{18}Cu_2I_2O_2S_2$ (687.30): C, 27.96; H, 2.64; S, 9.33. Found: C, 26.36; H, 2.35; S, 9.20%.
Polymer CP3. Yield (98%) Anal. Calcd. for $C_{118}H_{144}Cu_{14}I_{14}N_8O_{12}S_{12}$ (4917.28): C, 28.82; H, 2.95; S, 7.82. Found: C, 27.54; H, 2.72; S, 8.33 %.
Polymer CP3'. Yield (85%) Anal. Calcd. for $C_{37}H_{45}Cu_2I_2NO_4S_4$ (1076.91): C, 41.27; H, 4.21; S, 11.91; N 1.30%. Found: C, 39.2; H, 4.07; S, 12.12 %; N 1.94%.
Polymer CP5. Yield (90%) Anal. Calcd. for $C_{19}H_{24}Cu_2I_2O_2S_2$ (729.38): C, 31.29; H, 3.32; S, 8.79. Found: C, 37.81; H, 3.99; S, 10.55%.
Polymer CP6. Yield (98%) Anal. Calcd. for $C_{10}H_{13}CuIOS$ (371.70): C, 32.31; H, 3.53; S, 8.62. Found: C, 32.31; H, 3.74; S, 8.50%.
Polymer CP7. Yield (84%) Anal. Calcd. for $C_{21}H_{28}Cu_2I_2O_2S_2$ (371.72): C, 33.30; H, 3.73; S, 8.46. Found: C, 33.47; H, 3.58; S 7.32.
Polymer CP8. Yield (92%) Anal. Calcd. for $C_{11}H_{15}CuIOS$ (385.75): C, 34.25; H, 3.92; S, 8.31. Found: C, 38.48; H, 4.38; S, 9.44%.

Infrared and Raman

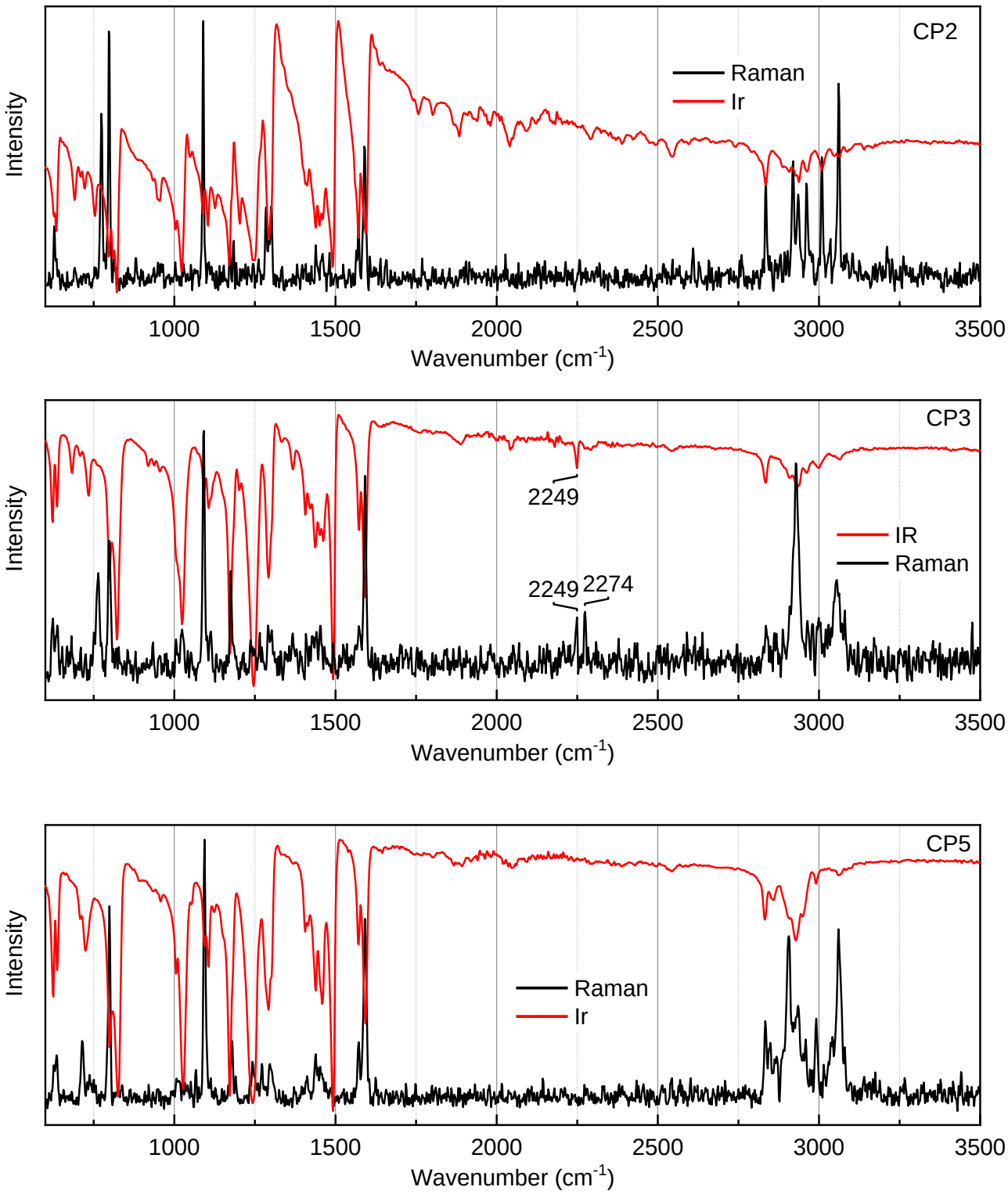

Figure S1. Solid state Raman and IR spectra of **CP2, CP3** and **CP5**.

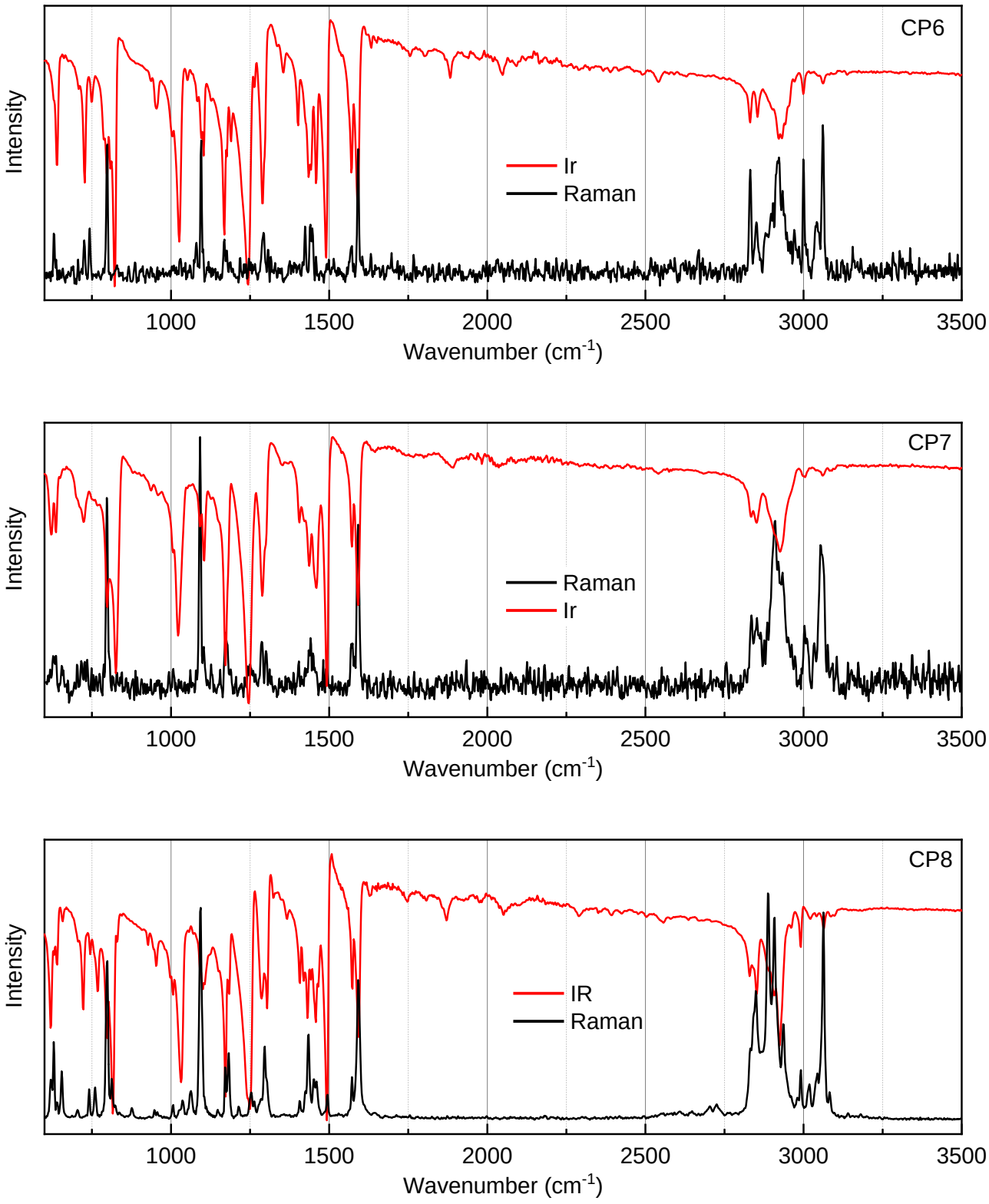

Figure S2. Solid state Raman and IR spectra of **CP6, CP7** and **CP8**.

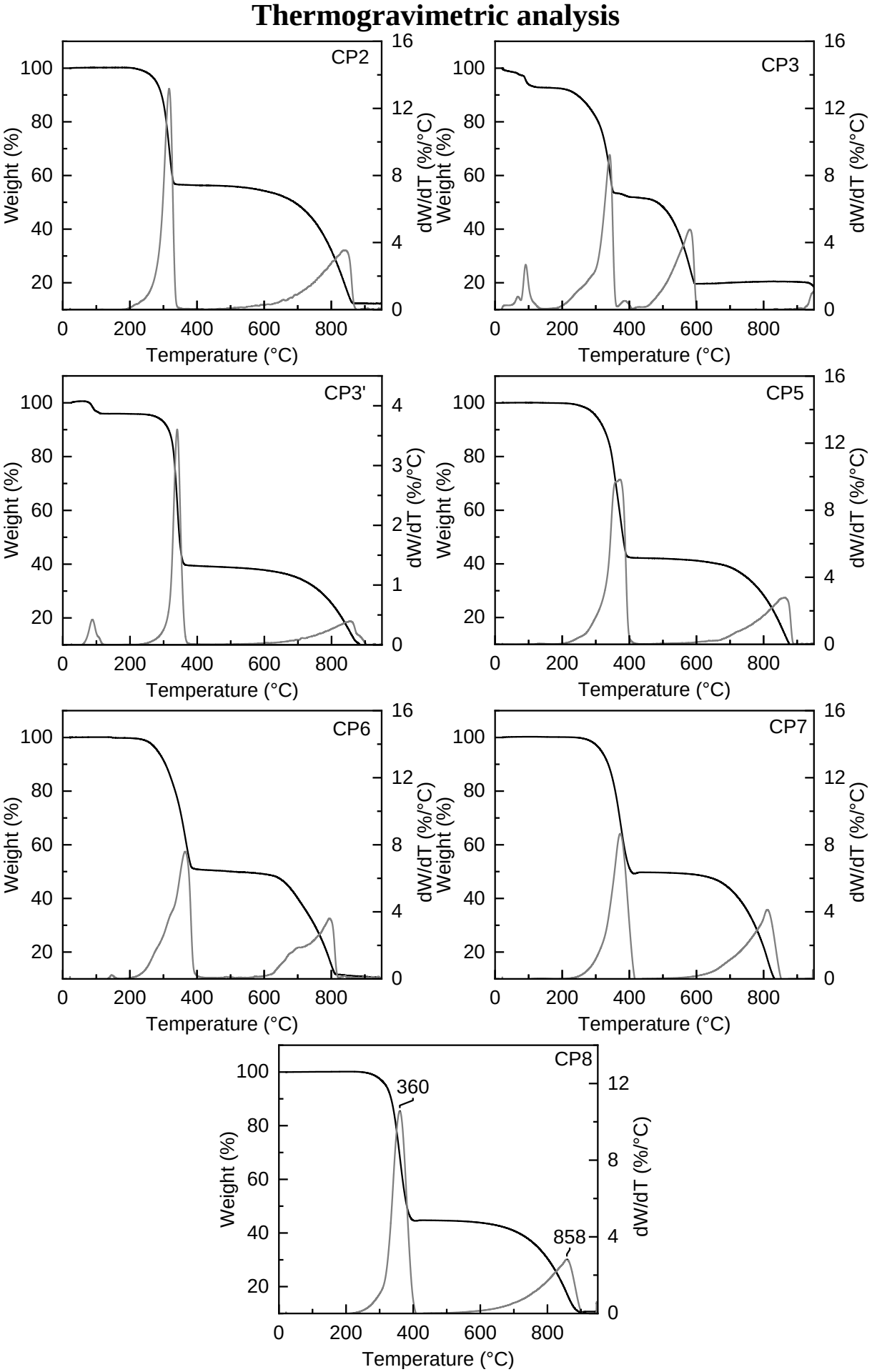

Figure S3. TGA (black) and first derivative (grey) traces of **CP2,3, 3'** and **CP5-8** under Ar(g).

Crystal Structures and data

Table S1. Crystal data, data collection, and structure refinement for **CP2** (123-298K).

Compound	**CP2 (123 K)**	**CP2 (173 K)**	**CP2 (223 K)**	**CP2 (298 K)**
Formula	$C_{16}H_{18}Cu_2I_2O_2S_2$	$C_{16}H_{18}Cu_2I_2O_2S_2$	$C_{16}H_{18}Cu_2I_2O_2S_2$	$C_{16}H_{18}Cu_2I_2O_2S_2$
Formula weight	687.30	687.30	687.30	687.30
Temperature/K	123	173	223	298
Wavelength/Å	0.71073	0.71073	0.71073	0.71073
Crystal system	monoclinic	monoclinic	monoclinic	monoclinic
Space group	*C* 2/*c*	*C* 2/*c*	*C* 2/*c*	*C* 2/*c*
a/Å	26.576(4)	26.630(3)	26.6121(12)	26.689(5)
b/Å	9.5840(11)	9.6328(9)	9.6449(4)	9.7011(18)
c/Å	7.8810(9)	7.8938(7)	7.8980(3)	7.9152(14)
a /°	90	90	90	90
β /°	99.586(6)	99.730(4)	99.7984(19)	100.175(8)
γ /°	90	90	90	90
Volume/ Å^3	1979.3(4)	1995.8(3)	1997.62(14)	2017.1(6)
Z	8	4	4	4
Density (calc.) g/cm^3	2.306	2.287	2.285	2.263
Absorption coefficient/mm^{-1}	5.486	5.440	5.435	5.383
F(000)	1304	1304.0	1304.0	1304.0
Crystal size/mm	0.404 × 0.144 × 0.078	0.404 × 0.144 × 0.078	0.404 × 0.144 × 0.078	0.404 × 0.144 × 0.078
2θ range for data collection/°	6.22 to 61.48	6.208 to 55.98	6.214 to 55.988	6.204 to 55.986
Index ranges	$-34 \le h \le 34$, $-10 \le k \le 10$, $-12 \le l \le 12$	$-35 \le h \le 35$, $-12 \le k \le 12$, $-10 \le l \le 10$	$-35 \le h \le 35$, $-12 \le k \le 12$, $-10 \le l \le 10$	$-35 \le h \le 35$, $-12 \le k \le 12$, $-10 \le l \le 10$
Reflections collected	33562	23410	40189	40277
Independent reflections	2397 [*R*(int) = 0.0382]	2413 [*R*(int) = 0.0574]	2416 [*R*(int) = 0.0497]	2443 [*R*(int) = 0.0643]
Refinement method	Full-matrix least-squares on F^2	Full-matrix least-squares on F^2	Full-matrix least-squares on F^2	Full-matrix least-squares on F^2
Data / restraints / parameters	2397/0/ 110	2413/0/ 110	2416/0/110	2443/0/110
Goodness-of-fit on F^2	1.089	1.065	1.064	1.043
Final *R* indices [$I > 2\sigma(I)$]	R_1 = 0.0142, wR_2 = 0.0306	R_1 = 0.0171, wR_2 = 0.0348	R_1 = 0.0162, wR_2 = 0.0358	R_1 = 0.0196, wR_2 = 0.0399
R indices (all data)	R_1 = 0.0170, wR_2 = 0.0313	R_1 = 0.0226, wR_2 = 0.0359	R_1 = 0.0197, wR_2 = 0.0367	R_1 = 0.0264, wR_2 = 0.0412
Largest diff. peak and hole/e. Å^{-3}	0.412 and -0.524	0.57 and -0.55	0.39 and -0.64	0.46 and -0.65

Table S2. Crystal data, data collection, and structure refinement for **CP3, CP3', CP5** and **CP6**.

Compound	**CP3**	**CP3'**	**CP5**	**CP6**
Formula	$C_{118}H_{144}Cu_{14}I_{14}N_8O_{12}S_{12}$	$C_{37}H_{45}Cu_2I_2NO_4S_4$	$C_{19}H_{24}Cu_2I_2O_2S_2$	$C_{10}H_{13}CuIOS$
Formula weight	4917.28	1076.86	729.38	371.70
Temperature/K	173(2)	173(2)	173(2)	173(2)
Wavelength/Å	0.71073	0.71073	0.71073	0.71073
Crystal system	monoclinic	triclinic	triclinic	monoclinic
Space group	*P* 1 2/*n* 1	*P* -1	*P* -1	*P* 1 2_1/*n* 1
a/Å	20.2112(7)	13.5982(17)	12.997(9)	12.2799(6)
b/Å	21.6942(7)	17.606(2)	14.422(9)	4.4770
c/Å	39.5341(13)	18.698(2)	14.631(10)	21.1329(2)
α/°	90	83.2730(10)	60.593(14)	90
β/°	90.2010(10)	73.2770(10)	82.60(2)	94.9460(10)
γ/°	90	80.5670(10)	89.146(16)	90
Volume/ $Å^3$	17334.2(10)	4217.6(9)	2366(3)	1157.50(6)
Z	4	4	4	4
Density (calc.) g/cm^3	1.884	1.696	2.048	2.133
Absorption coefficient/mm^{-1}	4.364	2.708	4.596	4.699
F(000)	9376	2136	1400	716
Crystal size/mm	0.290 × 0.400 × 0.650	0.230 × 0.312 × 0.420	0.230 × 0.390 × 0.540	0.130 × 0.295 × 0.800
θ range for data collection/°	1.72 to 26.77	1.14 to 26.53	1.58 to 26.45	1.85 to 26.73
Index ranges	$-25 \le h \le 25$, $-26 \le k \le 27$, $-49 \le l \le 49$	$-17 \le h \le 16$, $-23 \le k \le 23$, $-23 \le l \le 23$	$-16 \le h \le 16$, $-18 \le k \le 18$, $-18 \le l \le 18$	$-15 \le h \le 15$, $-5 \le k \le 5$, $-26 \le l \le 26$
Reflections collected	199048	115280	33513	14489
Independent reflections	36306 [*R*(int) = 0.0412]	17302 [*R*(int) = 0.0259]	9647 [*R*(int) = 0.0197]	2444 [*R*(int) = 0.0332]
Refinement method	Full-matrix least-squares on F^2	Full-matrix least-squares on F^2	Full-matrix least-squares on F^2	Full-matrix least-squares on F^2
Data / restraints / parameters	36306/0/1599	17302/0/911	9647/16/501	2444/0/128
Goodness-of-fit on F^2	1.057	1.237	1.066	1.365
Final *R* indices [$I > 2\sigma(I)$]	$R_1 = 0.0475$, $wR_2 = 0.1189$	$R_1 = 0.0331$, $wR_2 = 0.0621$	$R_1 = 0.0261$, $wR_2 = 0.0565$	$R_1 = 0.0307$, $wR_2 = 0.0700$
R indices (all data)	$R_1 = 0.0713$, $wR_2 = 0.1289$	$R_1 = 0.0504$, $wR_2 = 0.0741$	$R_1 = 0.0296$, $wR_2 = 0.0581$	$R_1 = 0.0315$, $wR_2 = 0.0702$
Largest diff. peak and hole/e. $Å^{-3}$	2.933 and -1.324	1.419 and -0.962	2.038 and -1.411	0.958 and -0.781

Table S3. Crystal data, data collection, and structure refinement for **CP8** at 100-293K.

Compound	**CP8 (100K)**	**CP8 (150K)**	**CP8 (173K)**	**CP8 (200K)**	**CP8 (250K)**	**CP8 (293K)**
Formula	$C_{11}H_{15}CuIOS$	$C_{11}H_{15}CuIOS$	$C_{22}H_{30}Cu_2I_2O_2S_2$	$C_{11}H_{15}CuIOS$	$C_{11}H_{15}CuIOS$	$C_{11}H_{15}CuIOS$
Formula weight	385.73	385.73	771.46	385.73	385.73	385.73
Temperature/K	100.03	150.12	173(2)	200.11	250.09	293.08
Wavelength/Å	0.71073	0.71073	0.71073	0.71073	0.71073	0.71073
Crystal system	tetragonal	tetragonal	tetragonal	tetragonal	tetragonal	tetragonal
Space group	$I\,4_1/a$	$I\,4_1/a$	$I\,4_1/a$	$I\,4_1/a$	$I\,4_1/a$	$I\,4_1/a$
a/Å	20.8973(13)	20.9498(14)	20.990(3)	20.9974(16)	21.041(3)	21.118(3)
b/Å	20.8973(13)	20.9498(14)	20.99	20.9974(16)	21.041(3)	21.118(3)
c/Å	11.6300(8)	11.6393(9)	11.6457(17)	11.6457(10)	11.6474(16)	11.6677(18)
α/°	90	90	90	90	90	90
β/°	90	90	90	90	90	90
γ/°	90	90	90	90	90	90
Volume/ Å^3	5078.8(7)	5108.4(8)	5130.9(10)	5134.5(9)	5156.8(15)	5203.7(16)
Z	16	16	8	16	16	16
Density (calc.) g/cm^3	2.018	2.006	1.997	1.996	1.987	1.969
Absorption coefficient/mm^{-1}	4.288	4.263	4.244	4.241	4.223	4.185
F(000)	2992.0	2992.0	2992	2992.0	2992.0	2992.0
Crystal size/mm	0.463 × 0.346 × 0.096	0.463 × 0.346 × 0.096	0.120 × 0.240 × 0.280	0.463 × 0.346 × 0.096	0.463 × 0.346 × 0.096	0.463 × 0.346 × 0.096
2θ range for data collection/°	5.592 to 72.828	5.582 to 72.782	5.48 to 53.14	5.572 to 72.79	5.566 to 72.896	6.76 to 72.8
Index ranges	$-34 \le h \le 34$, $-34 \le k \le 34$, $-19 \le l \le 19$	$-34 \le h \le 34$, $-34 \le k \le 34$, $-19 \le l \le 19$	$-26 \le h \le 25$, $-22 \le k \le 26$, $-13 \le l \le 14$	$-35 \le h \le 35$, $-35 \le k \le 35$, $-19 \le l \le 19$	$-35 \le h \le 35$, $-35 \le k \le 35$, $-19 \le l \le 19$	$-35 \le h \le 35$, $-35 \le k \le 35$, $-19 \le l \le 19$
Reflections collected	187640	188469	13971	189475	191605	186063
Independent reflections	6188 [R(int) = 0.0391]	6229 [R(int) = 0.0416]	2681 [R(int) = 0.0131]	6261 [R(int) = 0.0421]	6298 [R(int) = 0.0451]	6341 [R(int) = 0.0468]
Refinement method	Full-matrix least-squares on F^2	Full-matrix least-squares on F^2	Full-matrix least-squares on F^2	Full-matrix least-squares on F^2	Full-matrix least-squares on F^2	Full-matrix least-squares on F^2
Data / restraints / parameters	6188/0/137	6229/0/137	2681/0/137	6261/0/137	6298/0/137	6341/0/137
Goodness-of-fit on F^2	1.167	1.122	0.823	1.077	1.051	1.052
Final R indices [$I > 2\sigma(I)$]	R_1 = 0.0179, wR_2 = 0.0417	R_1 = 0.0208, wR_2 = 0.0487	R_1 = 0.0126, wR_2 = 0.0297	R_1 = 0.0211, wR_2 = 0.0520	R_1 = 0.0256, wR_2 = 0.0620	R_1 = 0.0278, wR_2 = 0.0686
R indices (all data)	R_1 = 0.0194, wR_2 = 0.0421	R_1 = 0.0235, wR_2 = 0.0496	R_1 = 0.0142, wR_2 = 0.0305	R_1 = 0.0254, wR_2 = 0.0538	R_1 = 0.0320, wR_2 = 0.0648	R_1 = 0.0368, wR_2 = 0.0732
Largest diff. peak and hole/e. Å^{-3}	1.03 and -1.21	0.91 and -1.17	0.301 and -0.268	0.85 and -1.21	0.94 and -1.11	0.94 and -1.02

Table S4. Comparison of the filled and void spaces.

CP	*T* (K)	Unit cell volume (Å³)[a]	Filled space per unit cell[a]	Void space per unit cell[a]
CP1		3853.80	754.29 Å³ (19.57%)	3099.51 Å³ (80.43%)
CP2	123	1979.30	373.08 Å³ (18.85%)	1606.22 Å³ (81.15%)
	173	1995.80	373.11 Å³ (18.69%)	1622.69 Å³ (81.31%)
	223	1997.62	373.06 Å³ (18.68%)	1624.55 Å³ (81.32%)
	298	2017.11	373.10 Å³ (18.50%)	1644.02 Å³ (81.50%)
CP3	173	17334.24	2557.17 Å³ (14.75%)	14777.08 Å³ (85.25%)
CP3'	173	4217.57	443.15 Å³ (10.51%)	3774.43 Å³ (89.49%)
CP4	100	1295.29	338.39 Å³ (26.12%)	956.90 Å³ (73.88%)
CP5	173	2365.51	366.52 Å³ (15.49%)	1998.99 Å³ (84.51%)
CP6	173	1157.47	187.56 Å³ (16.20%)	969.91 Å³ (83.80%)
CP7	173	4866.07	744.51 Å³ (15.30%)	4129.84 Å³ (84.87%)
CP8	100	5078.79	751.90 Å³ (14.80%)	4326.89 Å³ (85.20%)
	150	5108.42	751.91 Å³ (14.66%)	4356.51 Å³ (85.28%)
	173	5130.86	751.94 Å³ (14.66%)	4378.92 Å³ (85.34%)
	200	5134.48	751.93 Å³ (14.64%)	4382.28 Å³ (85.355)
	250	5156.58	751.89 Å³ (14.58%)	4404.69 Å³ (85.42%)
	293	5203.44	751.96 Å³ (14.45%)	4451.49 Å³ (85.55%)

[a] Calculated with Crystal Maker Software.

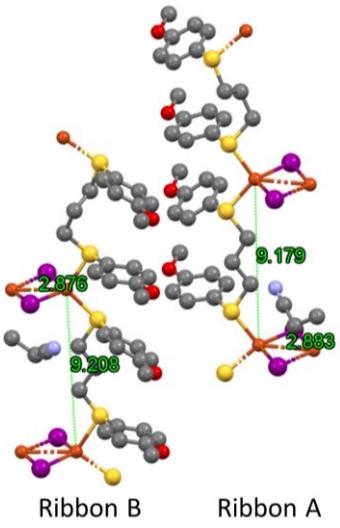

Figure S4. Fragment of the **CP3'** chain to show the EtCN molecules Color code: brown (Cu), purple (I), yellow (sulfur), red (oxygen), grey (carbon). The H-atoms are not shown for clarity.

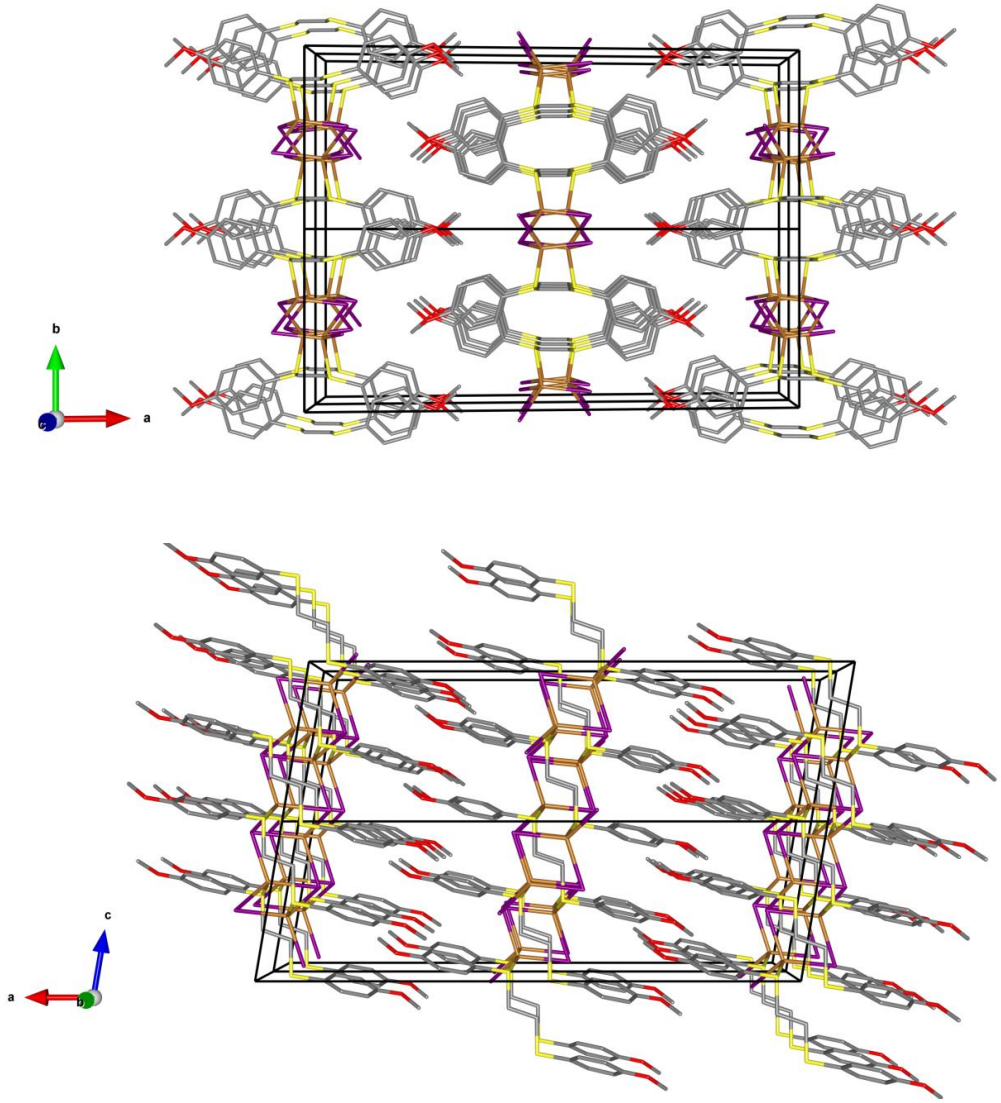

Figure S5. Two views of the stacking of **CP2**. The H-atoms are not shown for clarity. Color code: brown (Cu), purple (I), yellow (sulfur), red (oxygen), grey (carbon). The H-atoms are not shown for clarity.

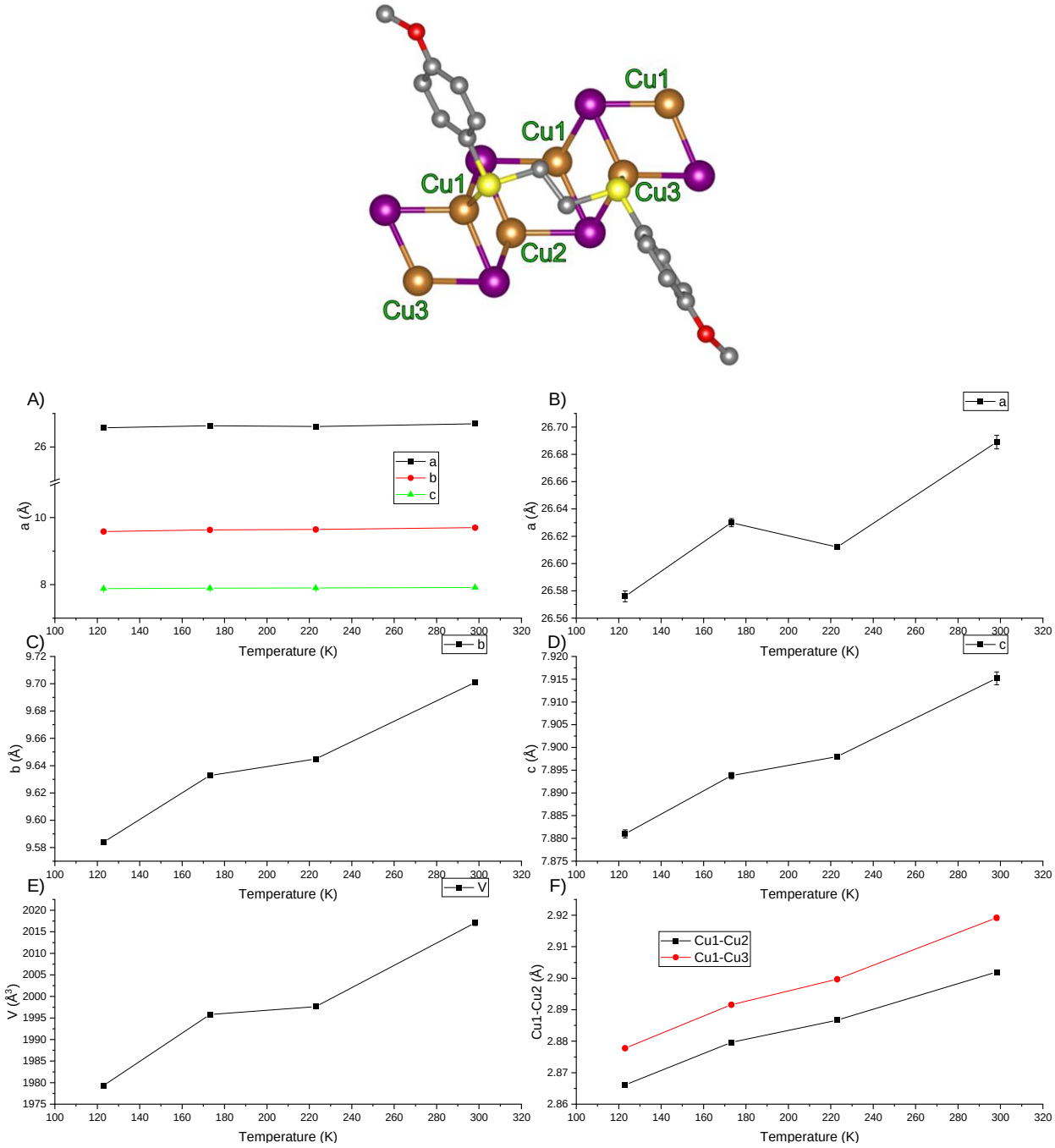

Figure S6. Temperature dependence of A), B), C), D) the unit cell parameters, E) volume and F) selected Cu-Cu distances of **CP2**.

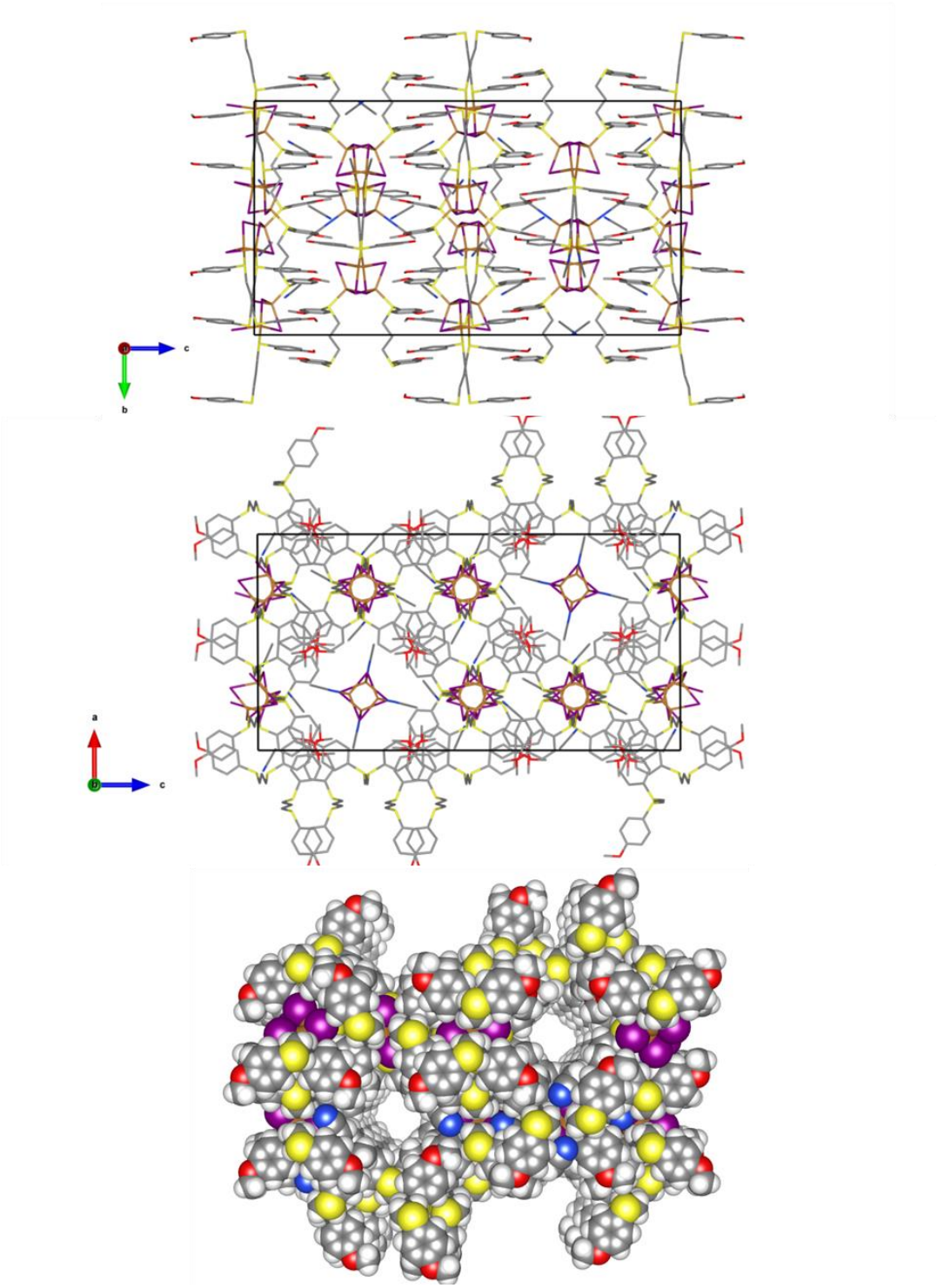

Figure S7. Stick representations showing the side (above) and top (middle) views of **CP3**. The H-atoms are not shown for clarity and the colour code is the same as Figure 3. Space filling image of **CP3** without the $Cu_4I_4(NCMe)_4$ clusters showing the channels.

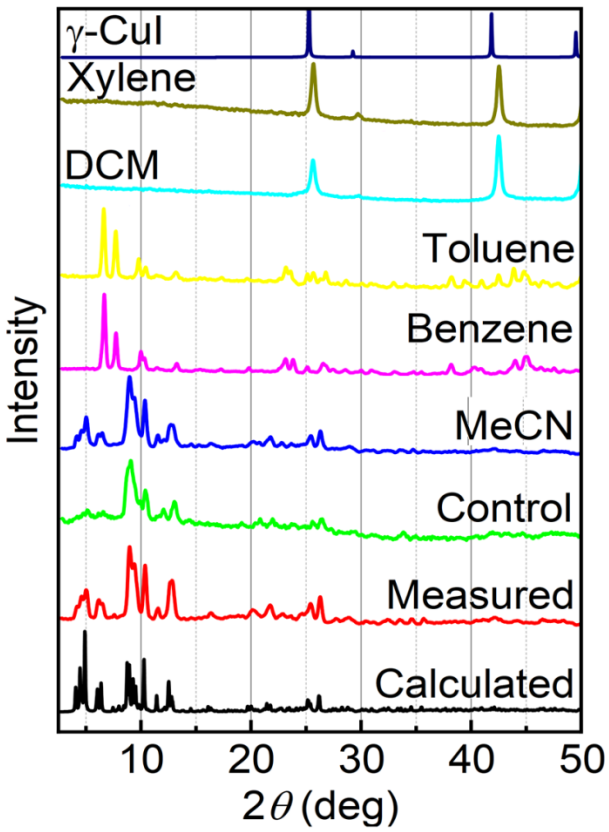

Figure S8. PXRD of **CP3** when exposed to various solvents, all of which do not dissolve **CP3** (navy blue = g-CuI; red = measured fresh after the reaction; light green = exposed to air for several weeks as a solid; blue (acetonitrile), turquoise (dichloromethane), purple (benzene), yellow (toluene), and dark green (xylene), exposed to a liquid for several weeks).

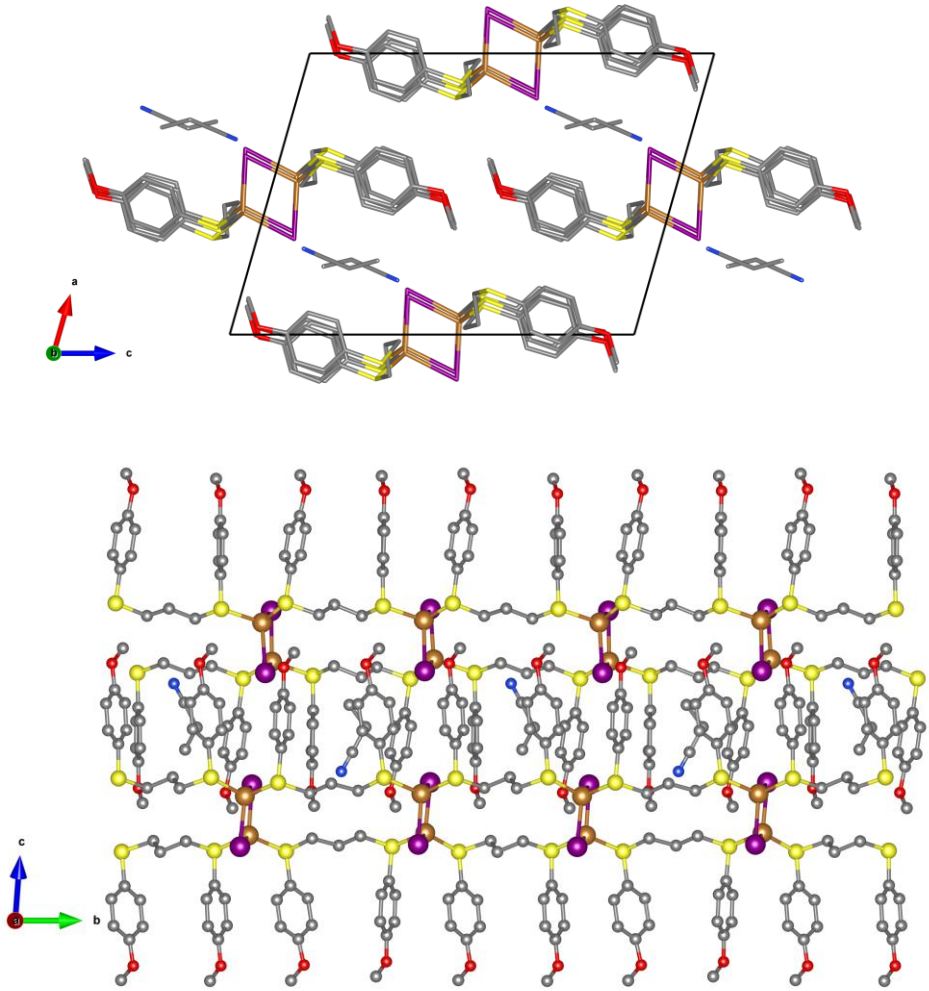

Figure S9. Two views of the stacking of **CP3'**. The H-atoms and PrCN molecules are not shown for clarity. Color code: brown (Cu), purple (I), yellow (sulfur), red (oxygen), grey (carbon). The H-atoms are not shown for clarity.

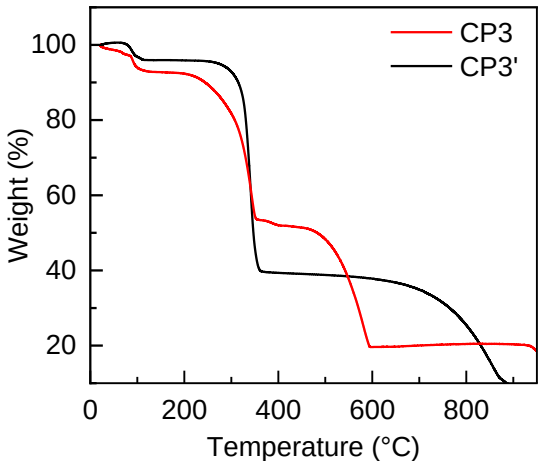

Figure S10. Comparison of the TGA traces of **CP3** (red) and **CP3'** (black) under Ar(g).

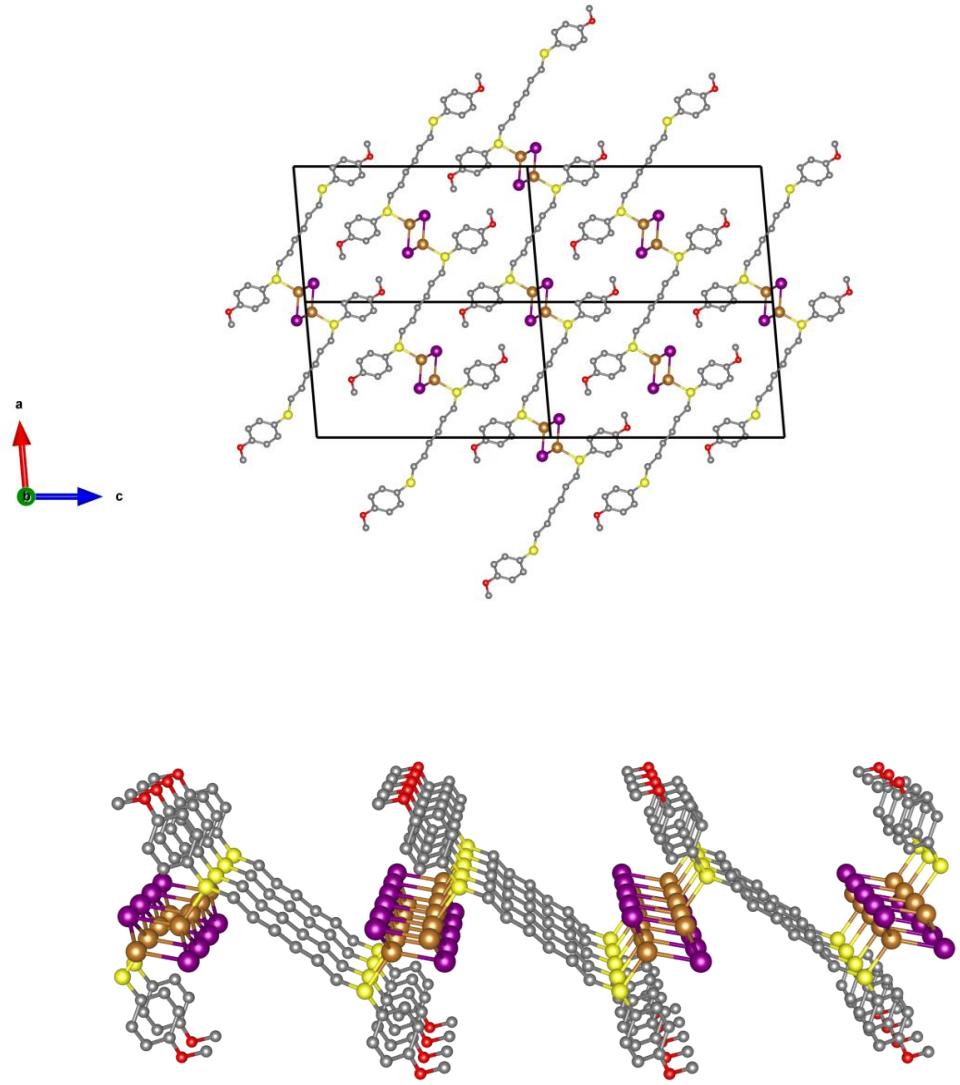

Figure S11. Two views of the stacking of **CP6**. The H-atoms are not shown for clarity. Color code: brown (Cu), purple (I), yellow (sulfur), red (oxygen), grey (carbon). The H-atoms are not shown for clarity.

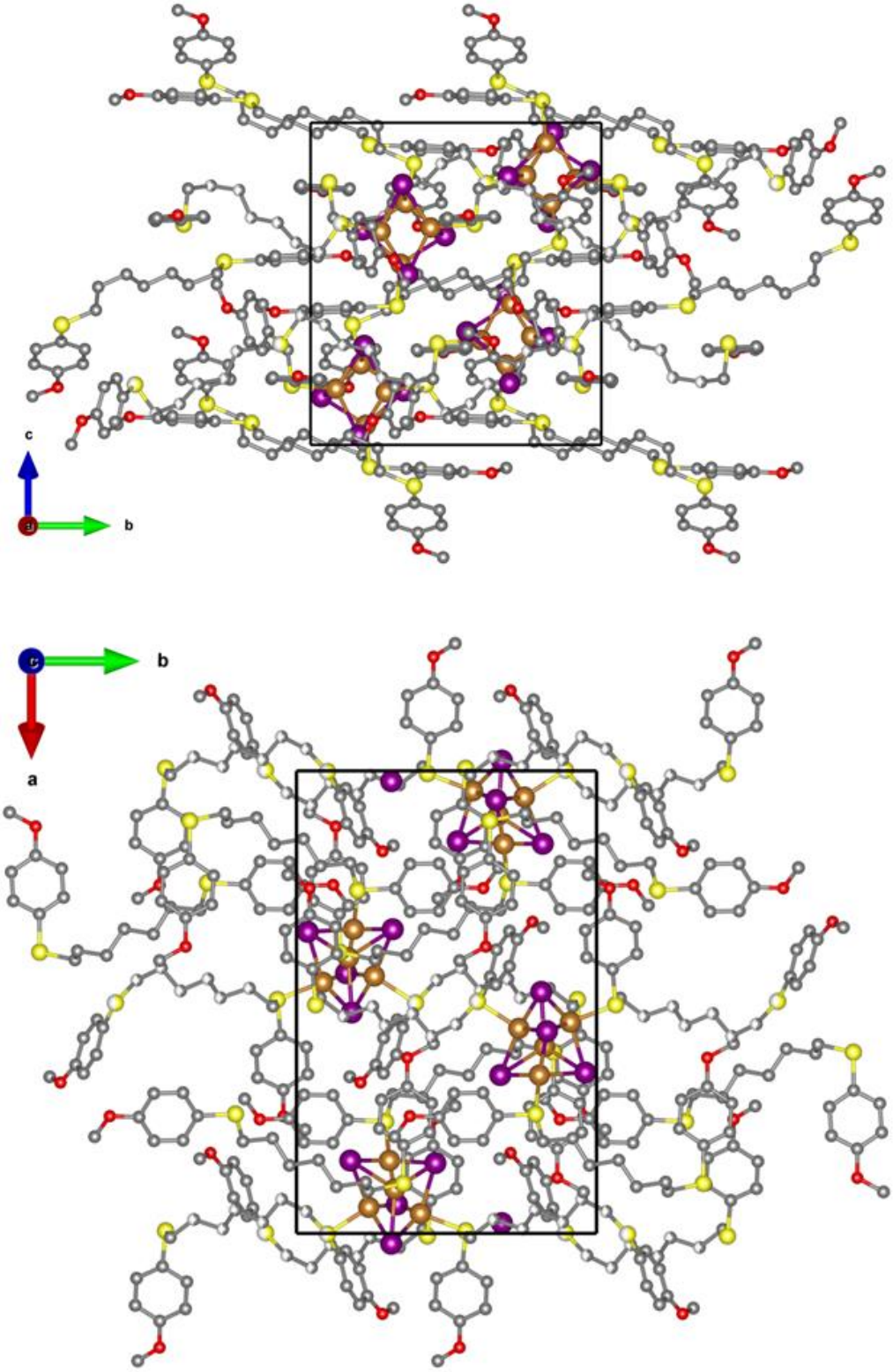

Figure S12. Two views of stacking of **CP7** (calculated structure).

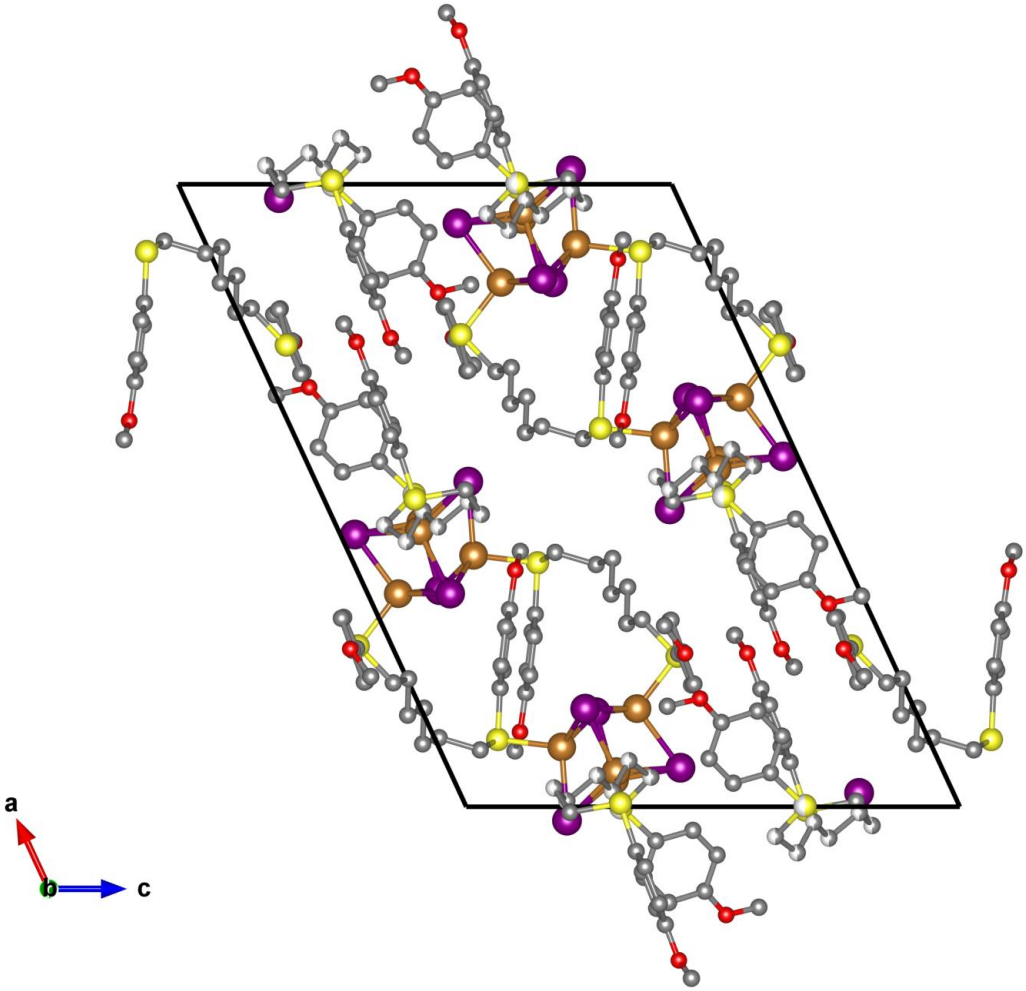

Figure S13. Another view of the stacking of **CP7** (calculated structure).

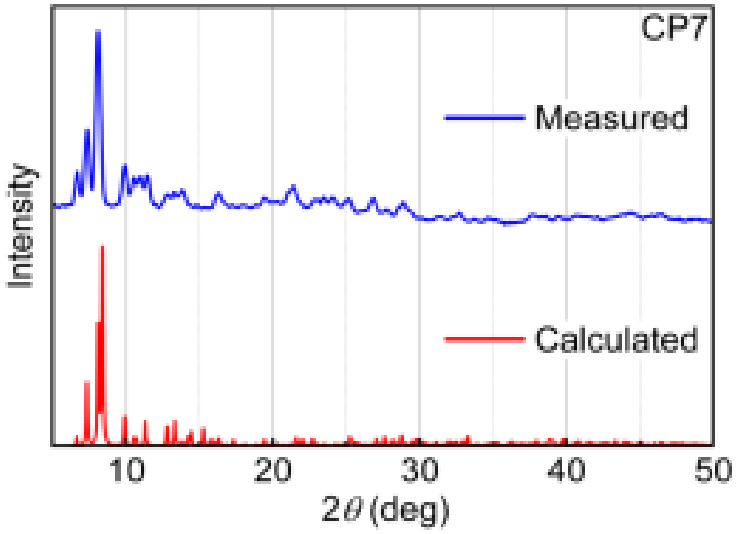

Figure S14. Comparison of the simulated PXRD pattern (red) from a calculated model of **CP7** (1D-$[(Cu_4I_4)(\mathbf{L7})]_n$) and the experimental one.

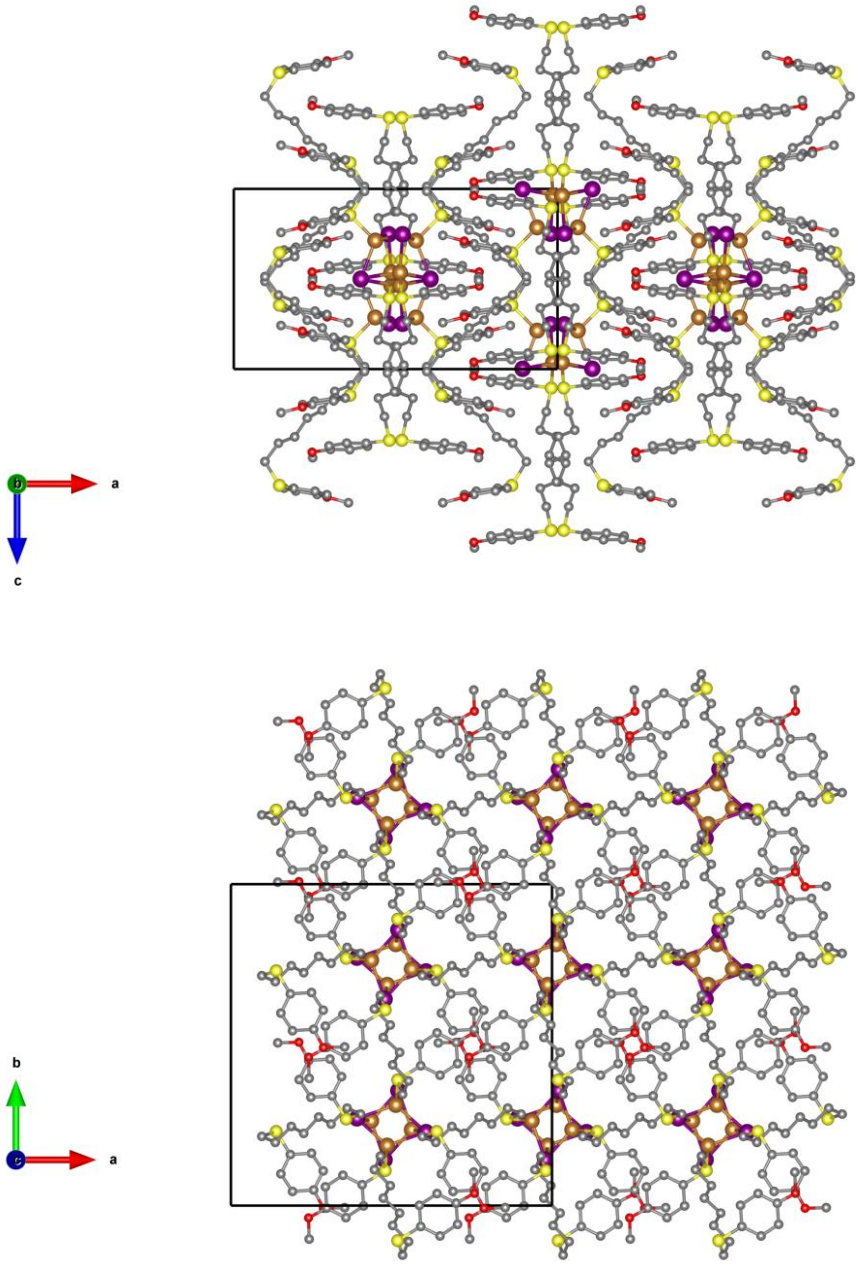

Figure S15. Two views of the stacking of **CP8**. The H-atoms are not shown for clarity. Color code: brown (Cu), purple (I), yellow (sulfur), red (oxygen), grey (carbon). The H-atoms are not shown for clarity.

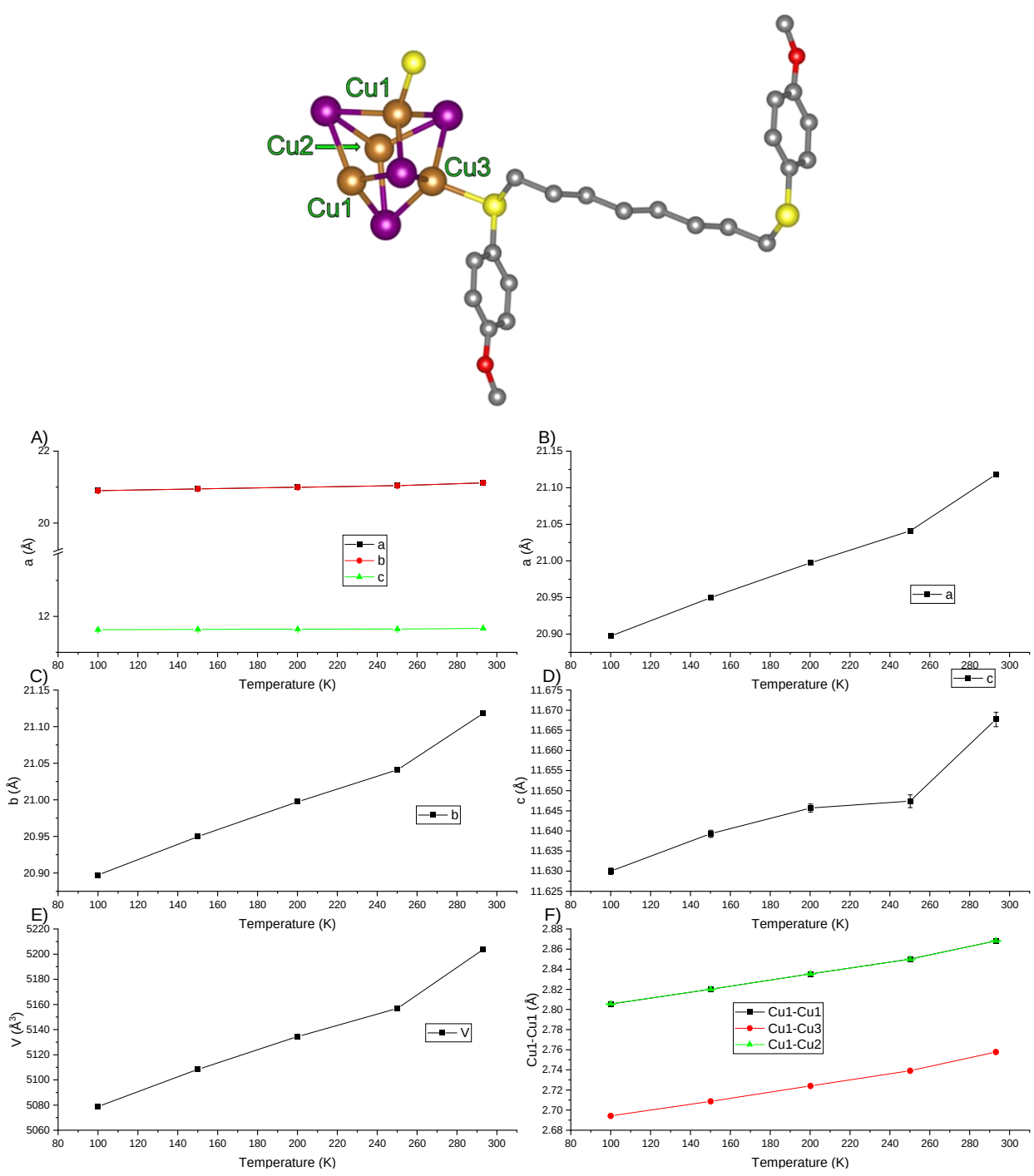

Figure S16. Temperature dependence of the A), B), C) D) unit cell parameters, E) volume and F) selected Cu-Cu distances of **CP8**.

Absorption, Excitation and Emission

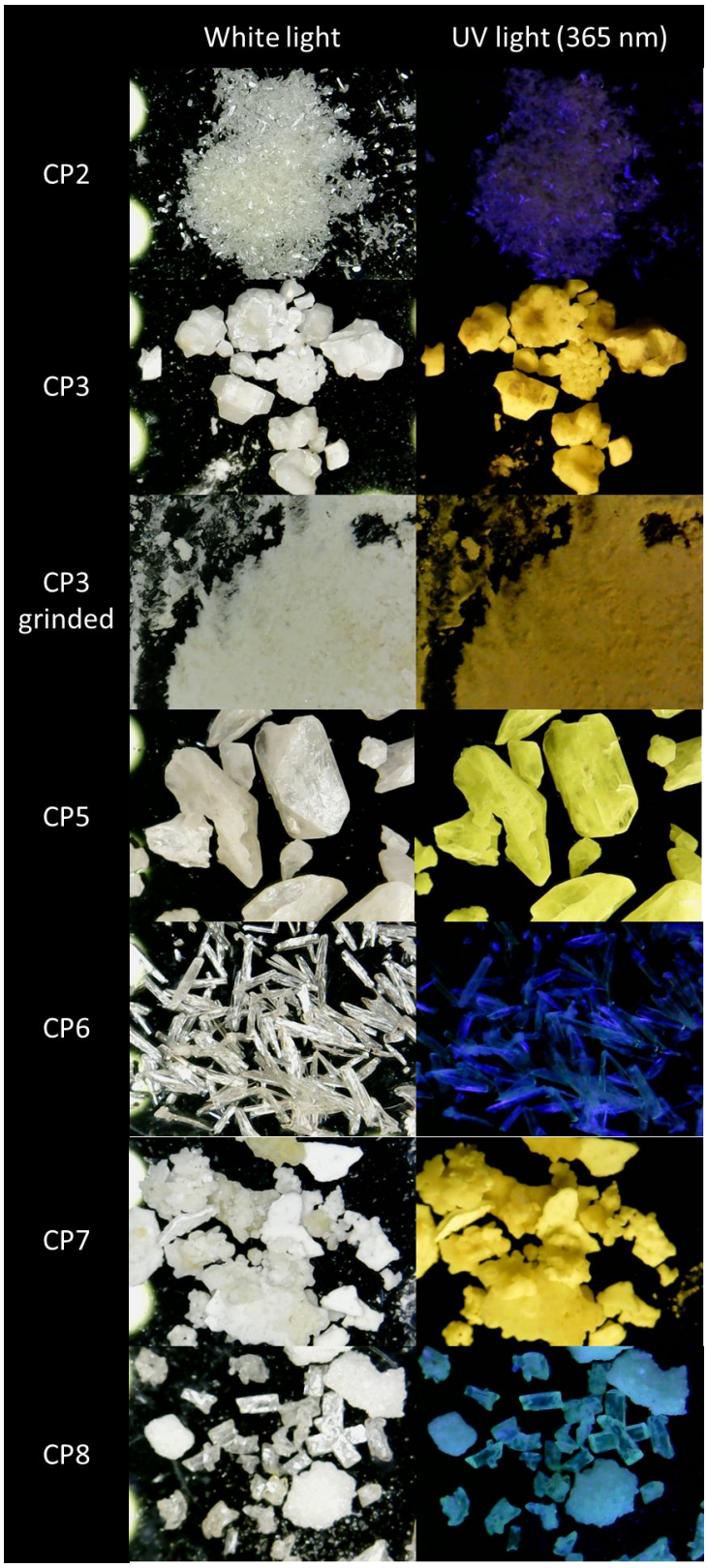

Figure S17. Photographs of the crystalline samples under white light (left) and UV lamp (λ_{exc} =365 nm; right).

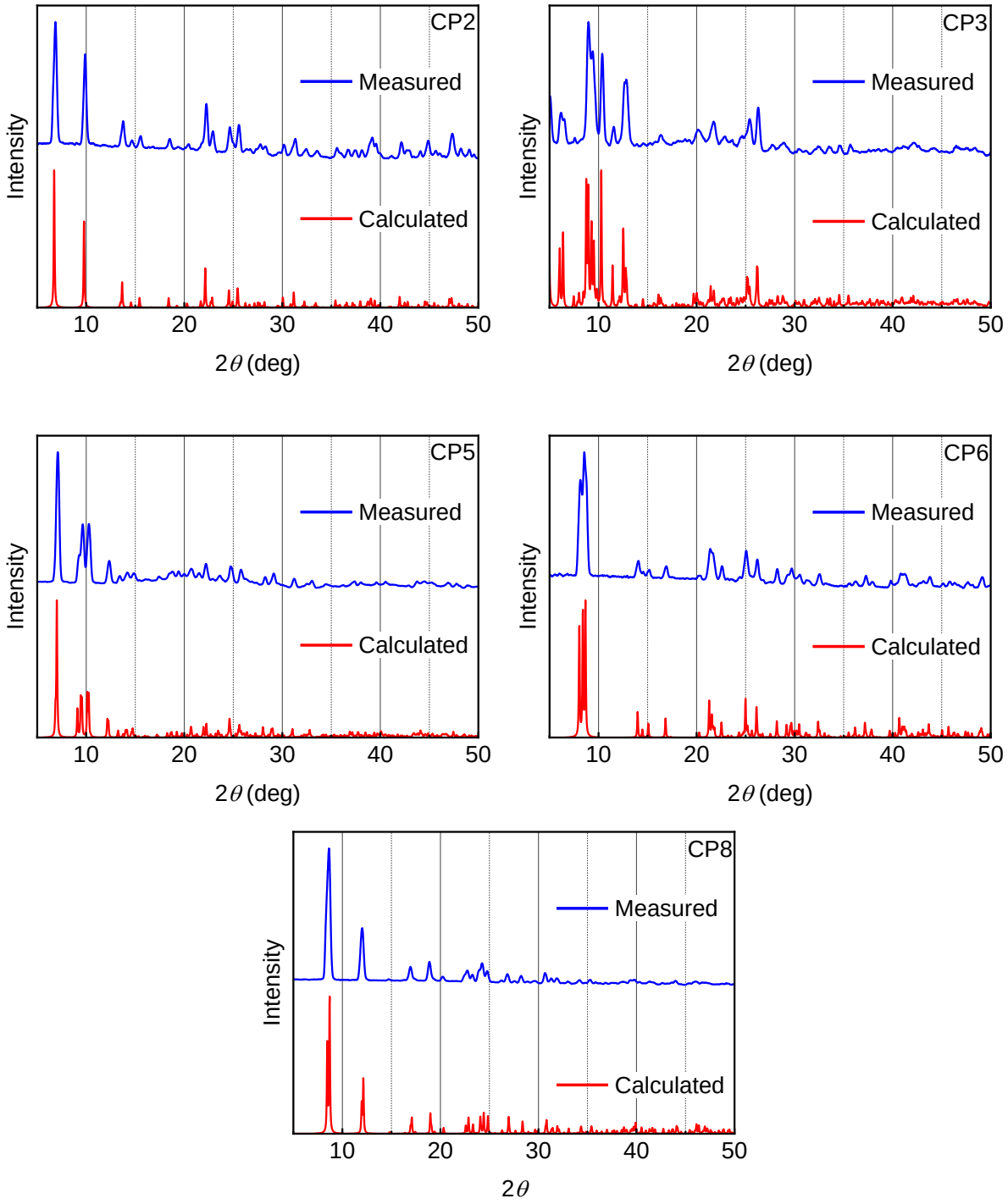

Figure S18. Powder X-ray diffraction patterns calculated (red) and experimental (blue) for **CP2, CP3, CP5, CP6** and **CP8** at 173 K. The calculated and measured diffraction patterns match well with each other, confirming the homogeneity of the crystalline phases.

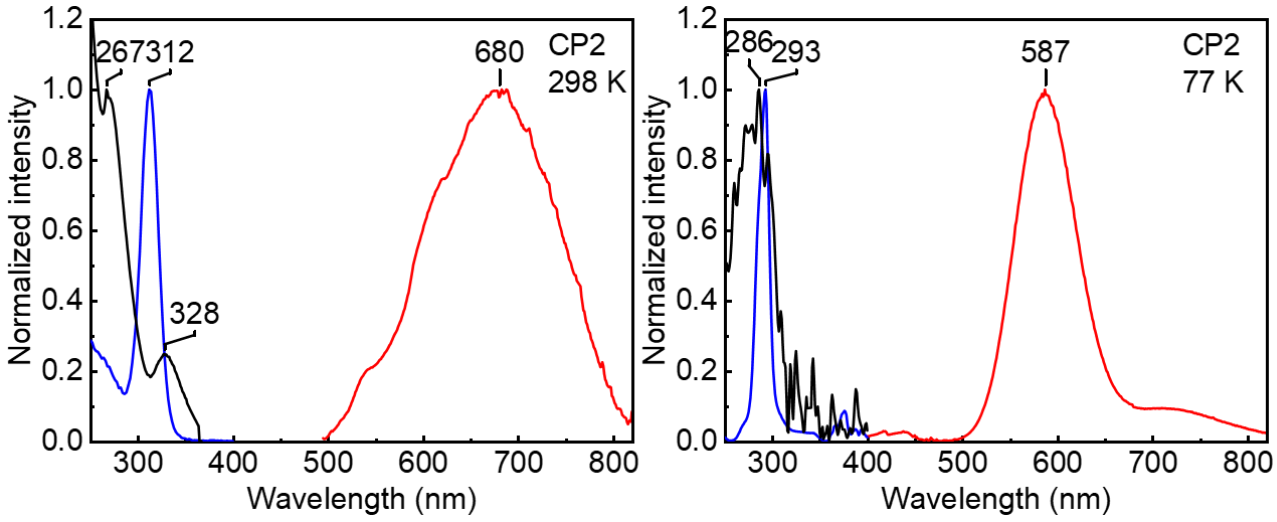

Figure S19. Solid-state absorption (black), emission (red) and excitation (blue) spectra of **CP2** at 298 K (λ_{ex} = 310 nm, λ_{em} = 680 nm) and 77K (λ_{ex} = 290 nm, λ_{em} = 585 nm).

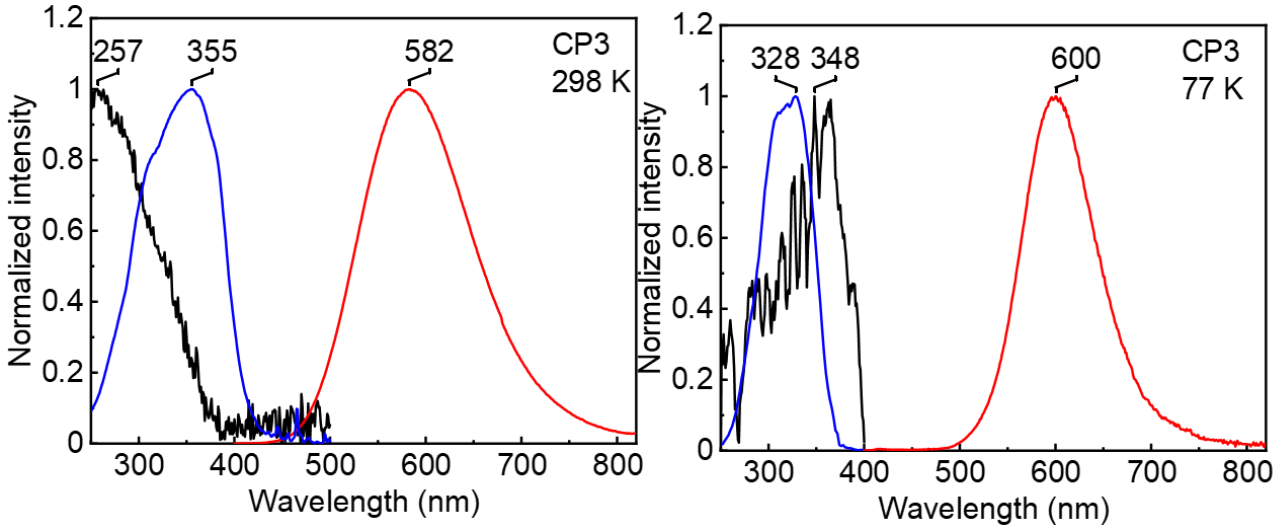

Figure S20. Solid-state absorption (black), emission (red) and excitation (blue) spectra of **CP3** at 298 K (λ_{ex} = 350 nm, λ_{em} = 580 nm) and 77K (λ_{ex} = 345 nm, λ_{em} = 600 nm).

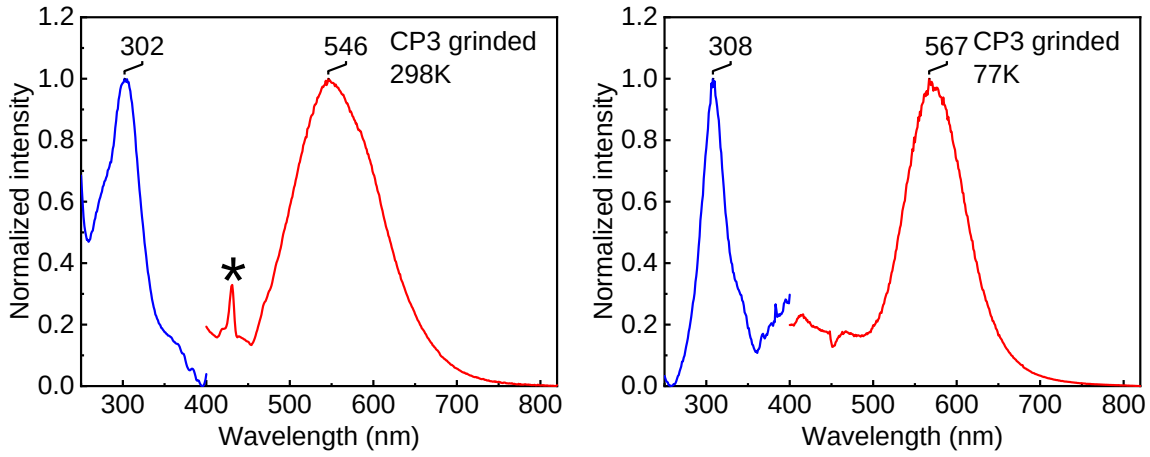

Figure S21. Solid-state emission (red) and excitation (blue) spectra of **grinded CP3** at 298 K (λ_{ex} = 350 nm, λ_{em} = 580 nm) and 77K (λ_{ex} = 345 nm, λ_{em} = 600 nm). * = artifact from light scattering diffusion.

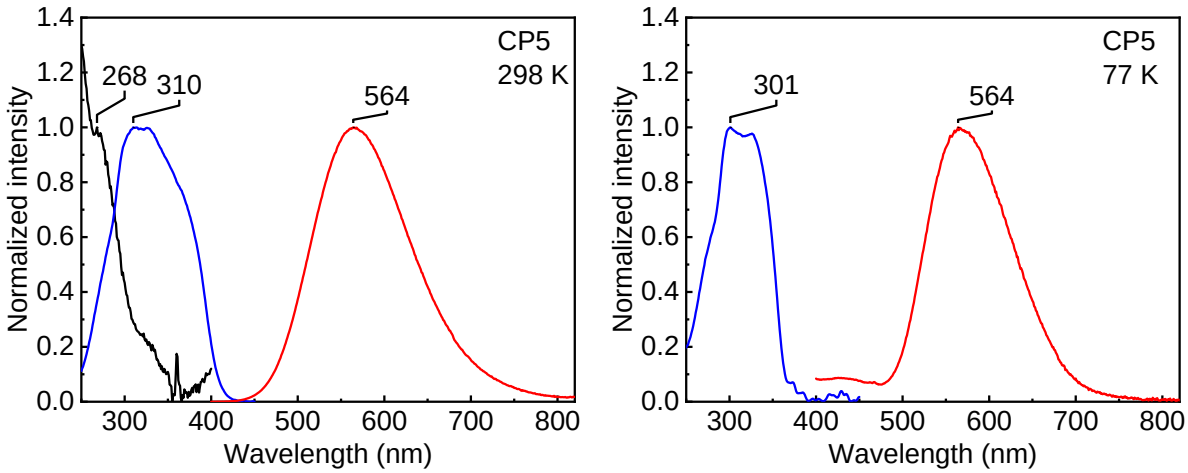

Figure S22. Solid-state absorption (black), emission (red) and excitation (blue and green) spectra of **CP5** at 298 K (λ_{ex} = 310 nm, λ_{em} = 560 nm) and 77K (λ_{ex} = 300 nm, λ_{em} = 565 nm).

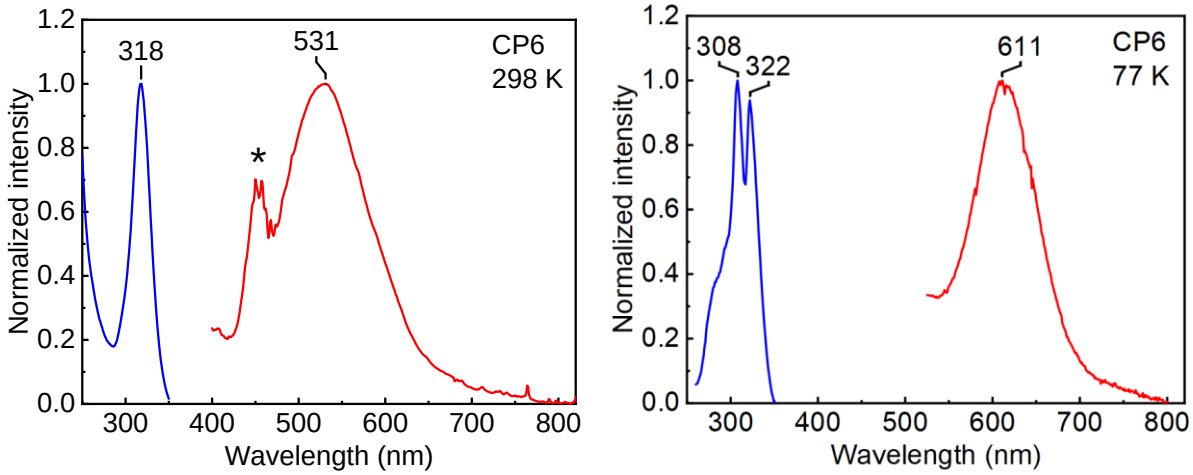

Figure S23. Solid-state emission (red) and excitation (blue) spectra of **CP6** at 298 K (left, λ_{ex} = 318 nm, λ_{em} = 530 nm. * = artifact from capillary sample holder) and at 77 K (right).

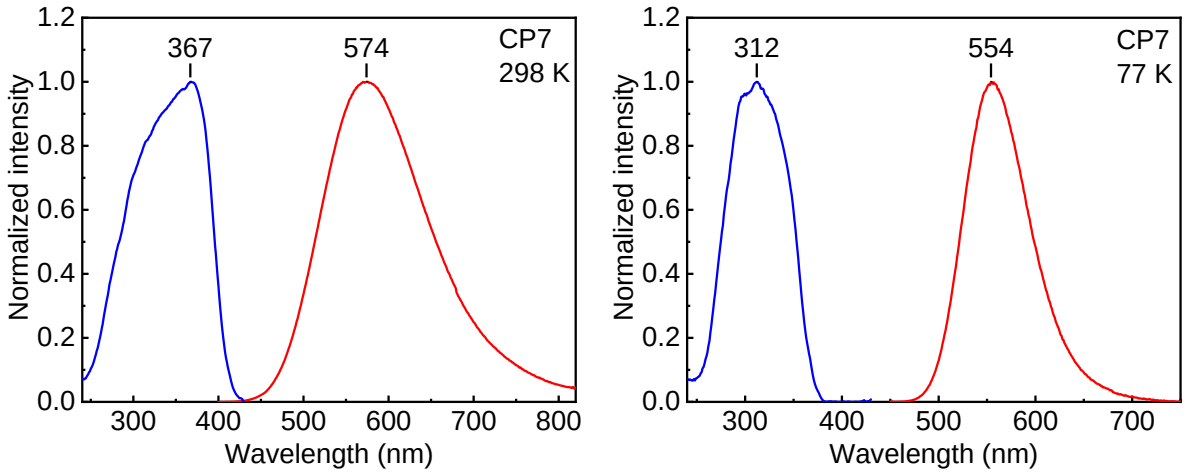

Figure S24. Solid-state emission (red) and excitation (blue) spectra of **CP7** at 298 K (λ_{ex} = 360 nm, λ_{em} = 570 nm) and 77K (λ_{ex} = 310 nm, λ_{em} = 555 nm).

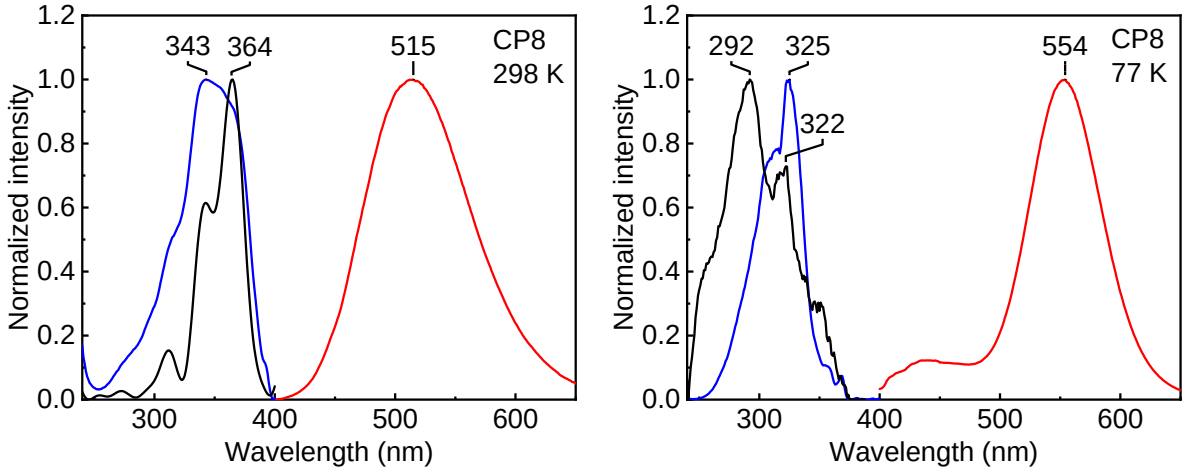

Figure S25. Solid-state absorption (black), emission (red) and excitation (blue) spectra of **CP8** at 298 K (λ_{ex} = 350 nm, λ_{em} = 515 nm) and 77K (λ_{ex} = 320 nm, λ_{em} = 555 nm).

Emission lifetimes

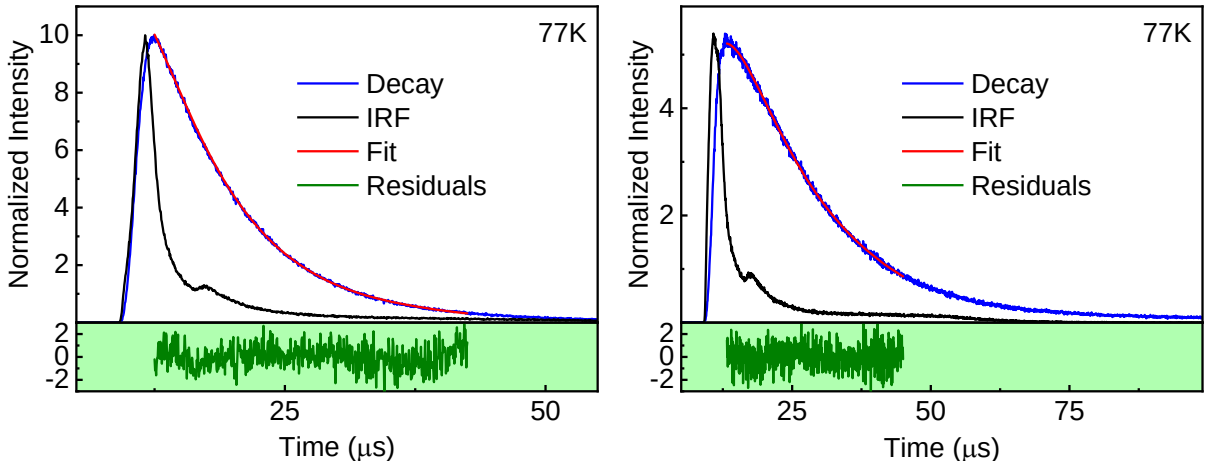

Figure S26. Decay of emission intensity, fit, IRF and residual of **CP2** at 77 K. Left, for **CP2** λ = 587 nm (λ_{ex} = 290 nm), τ_e {B} = 5.98 μs {0.0408}, χ^2 = 1.02. Right, for **CP2** λ_{emi} = 750 nm (λ_{exc} = 290 nm), τ_e {B}= 14.98 μs {0.0223}, χ^2 = 1.07.

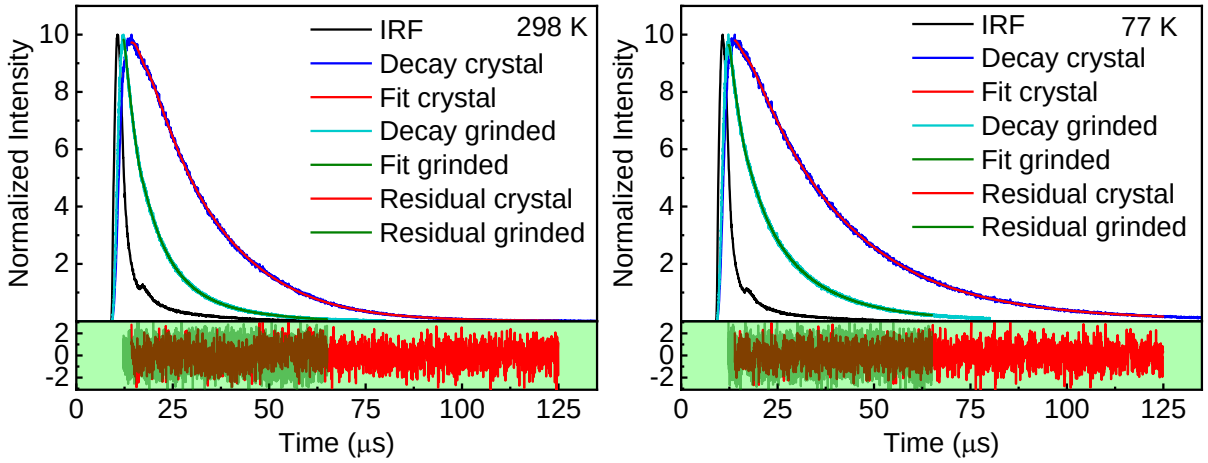

Figure S27. Decay of emission intensity, fit, IRF and residual of **CP3** and grinded **CP3**. Left, at 298 K, for **CP3** λ_{emi} = 580 nm (λ_{exc} = 355 nm), τ_e {B}= 0.45 μs {0.0202}, τ_e {B}= 6.53 μs {0.0070}, τ_e {B}= 15.22 μs {0.0138}, χ^2 = 1.02. For grinded **CP3** λ_{exc} = 550 nm (λ_{exc} = 300 nm), τ_e {B}= 0.32 μs {0.0051}, τ_e {B}= 2.31 μs {0.0037}, τ_e {B}= 7.73 μs {0.0020}, χ^2 = 0.99. Right, at 77 K, for **CP3** λ = 600 nm (λ_{ex} = 328 nm), τ_e {B} = 2.52 μs {0.0027}, τ_e {B}= 10.37 μs {0.0089}, τ_e {B}= 26.59 μs {0.0100}, χ^2 = 0.96. For grinded **CP3** λ_{emi} = 570 nm (λ_{exc} = 310 nm), τ_e {B}= 0.29 μs {0.0081}, τ_e {B}= 2.88 μs {0.0028}, τ_e {B}= 11.16 μs {0.0019}, χ^2 = 0.98.

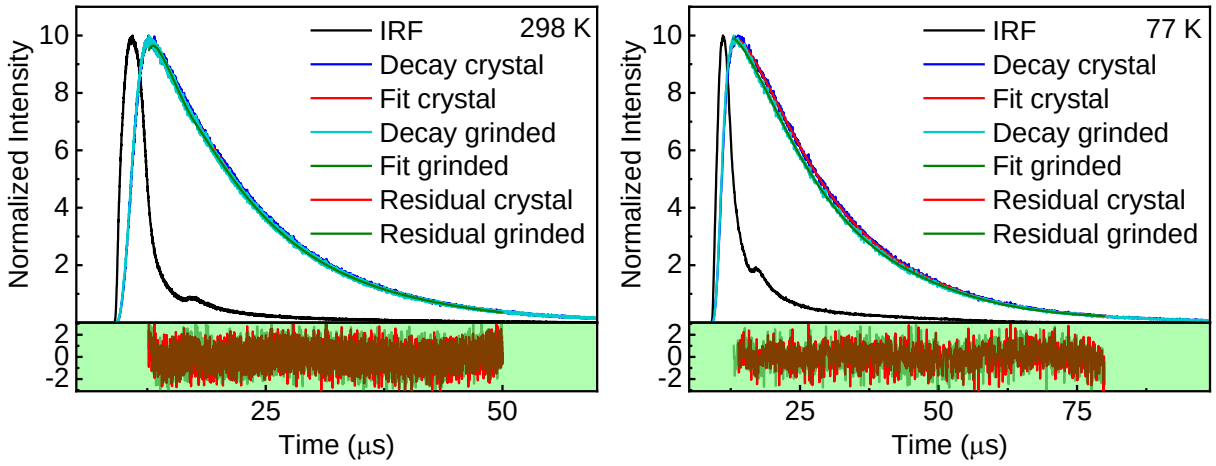

Figure S28. Decay of emission intensity, fit, IRF and residual of **CP5** and grinded **CP5**. Left, at 298 K, for **CP5** λ_{emi} = 560 nm (λ_{exc} = 310 nm), τ_e {B}= 7.47 μs {0.0048}, χ^2 = 0.98. For grinded **CP5** λ = 560 nm (λ_{ex} = 310 nm), τ_e {B}= 5.70 μs {0.0055}, χ^2 = 1.09. Right, at 77 K, for **CP5** λ_{emi} = 564 nm (λ_{exc} = 300 nm), τ_e {B}= 15.14 μs {0.0166}, χ^2 = 1.00. For **CP5** grinded λ = 564 nm (λ_{ex} = 300 nm), τ_e {B}= 14.91 μs {0.0174}, χ^2 = 1.04.

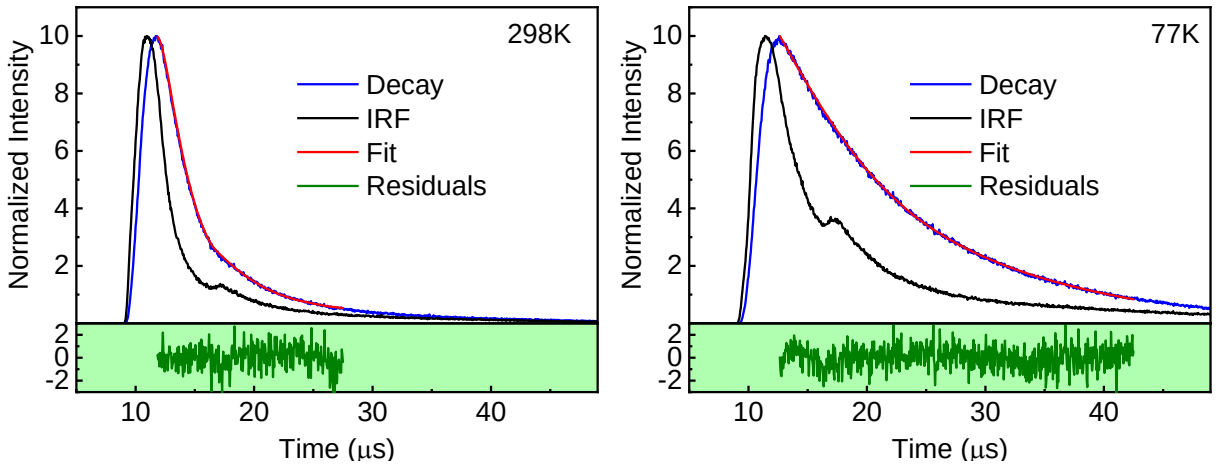

Figure S29. Decay of emission intensity (blue), fit (red), IRF (black) and residual (green) of **CP6**. Left, at 298 K, λ = 531 nm (λ_{ex} = 318 nm), τ_e {B}= 1.46 μs {0.0483}, χ^2 = 1.06. Right, at 77 K, λ = 612 nm (λ_{ex} = 318 nm), τ_e {B} = 6.29 μs {0.0262}, χ^2 = 1.00.

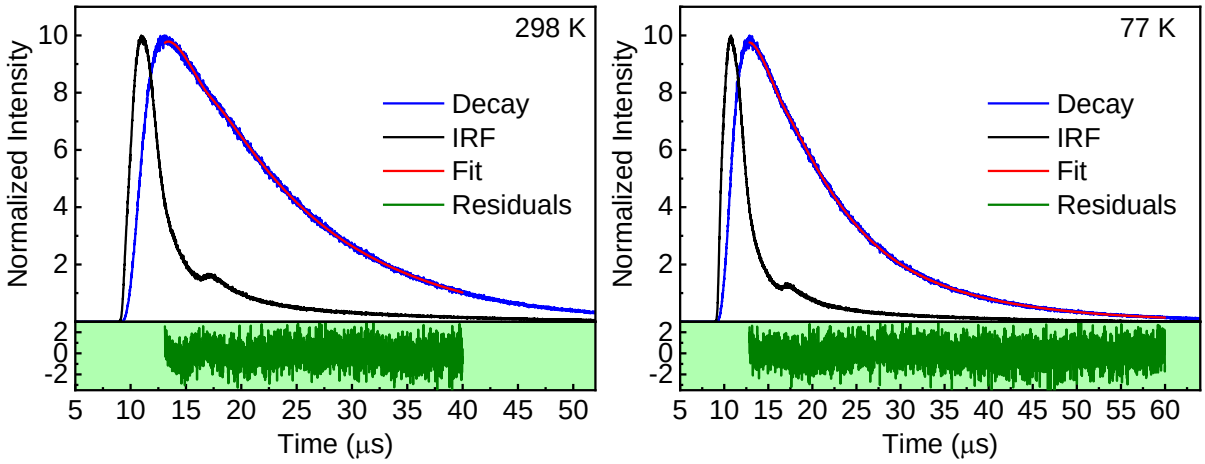

Figure S30. Decay of emission intensity (blue), fit (red), IRF (black) and residual (green) of **CP7**. Left, at 298 K, λ = 575 nm (λ_{ex} = 360 nm), τ_e {B}= 5.03 μs {0.0059}, χ^2 = 1.03. Right, at 77 K, λ = 555 nm (λ_{ex} = 312 nm), τ_e {B} = 5.99 μs {0.0021}, χ^2 = 1.03.

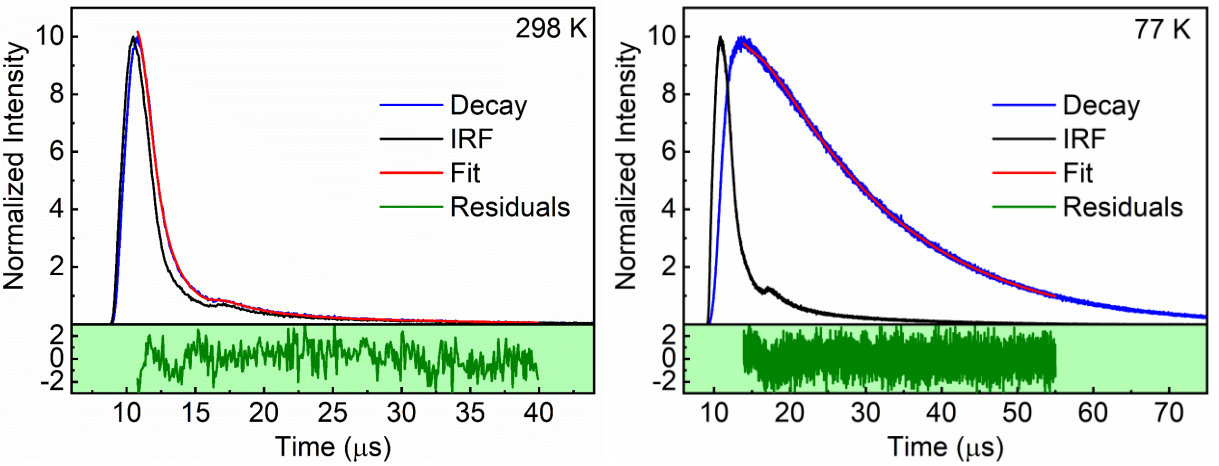

Figure S31. Decay of emission intensity (blue), fit (red), IRF (black) and residual (green) of **CP8**. Left, at 298 K, λ = 515 nm (λ_{ex} = 360 nm), τ_e {B}= 0.60 μs {0.1562}, χ^2 = 1.05. Right, at 77 K, λ = 554 nm (λ_{ex} = 320 nm), τ_e {B} = 13.37 μs {0.0041}, χ^2 = 1.02.

References

(1) Dolomanov, O. V.; Bourhis, L. J.; Gildea, R. J.; Howard, J. A. K.; Puschmann, H. OLEX2: A Complete Structure Solution, Refinement and Analysis Program. *J. Appl. Crystallogr.* **2009**, *42* (2), 339–341. https://doi.org/10.1107/S0021889808042726.

(2) Sheldrick, G. M. A Short History of SHELX. *Acta Crystallogr. Sect. A Found. Crystallogr.* **2008**, *64* (1), 112–122. https://doi.org/10.1107/S0108767307043930.

(3) Sheldrick, G. M. Crystal Structure Refinement with SHELXL. *Acta Crystallogr. Sect. C Struct. Chem.* **2015**, *71* (1), 3–8. https://doi.org/10.1107/S2053229614024218.

(4) Fullprof Homepage https://www.ill.eu/sites/fullprof/php/programsdccc.html?pagina=Treor90 (accessed Mar 15, 2022).

(5) Rodríguez-Carvajal, J. Recent Advances in Magnetic Structure Determination by Neutron Powder Diffraction. *Phys. B Condens. Matter* **1993**, *192* (1–2), 55–69. https://doi.org/10.1016/0921-4526(93)90108-I.

(6) Hartley, F. R.; Murray, S. G.; Levason, W.; Soutter, H. E.; McAuliffe, C. A. Systematics of Palladium(II) and Platinum(II) Dithioether Complexes. The Effect of Ligand Structure upon the Structure and Spectra of the Complexes and upon Inversion at Coordinated Sulphur. *Inorganica Chim. Acta* **1979**, *35* (C), 265–277. https://doi.org/10.1016/S0020-1693(00)93450-9.

(7) Schlachter, A.; Tanner, K.; Scheel, R.; Karsenti, P. L.; Strohmann, C.; Knorr, M.; Harvey, P. D. A Fused Poly(Truncated Rhombic Dodecahedron)-Containing 3D Coordination Polymer: A Multifunctional Material with Exceptional Properties. *Inorg. Chem.* **2021**, *60* (17), 13528–13538. https://doi.org/10.1021/acs.inorgchem.1c01856.

(8) Harvey, P. D.; Bonnot, A.; Lapprand, A.; Strohmann, C.; Knorr, M. Coordination RC6H4S(CH2)8SC6H4R/(CuI)n Polymers (R (n) = H (4); Me (8)): An Innocent Methyl Group That Makes the Difference. *Macromol. Rapid Commun.* **2015**, *36* (7), 654–659. https://doi.org/10.1002/marc.201400659.

(9) Knorr, M.; Khatyr, A.; Dini Aleo, A.; El Yaagoubi, A.; Strohmann, C.; Kubicki, M. M.; Rousselin, Y.; Aly, S. M.; Fortin, D.; Lapprand, A.; Harvey, P. D. Copper(I) Halides (X = Br, I) Coordinated to Bis(Arylthio)Methane Ligands: Aryl Substitution and Halide Effects on the Dimensionality, Cluster Size, and Luminescence Properties of the Coordination Polymers. *Cryst. Growth Des.* **2014**, *14* (11), 5373–5387. https://doi.org/10.1021/cg500905z.